DEVELOPMENT AND EVALUATION OF A MINOR GROOVE BINDER-TAQMAN RT-PCR ASSAY FOR THE DETECTION OF HUMAN RHINOVIRUS IN NASAL ASPIRATE SPECIMENS

by

Duc Hoang Do

B.S., University of Pittsburgh, 2001

Submitted to the Graduate Faculty of

The Graduate School of Public Health in partial fulfillment

of the requirements for the degree of

Master of Science

University of Pittsburgh

2005

UNIVERSITY OF PITTSBURGH

GRADUATE SCHOOL OF PUBLIC HEALTH

This thesis was presented

by

Duc Hoang Do

It was defended on

July 18, 2005

and approved by

Graduate Thesis Advisor:
Robert M. Wadowsky, Sc.D.
Professor
Departments of Pathology and Infectious Diseases and Microbiology
School of Medicine and Graduate School of Public Health
University of Pittsburgh

Committee Member:
Lee H. Harrison, M.D.
Professor
Departments of Epidemiology and Medicine
Graduate School of Public Health and School of Medicine
University of Pittsburgh

Committee Member:
Frank J. Jenkins, Ph.D.
Associate Professor
Departments of Pathology, Infectious Diseases and Microbiology, and the Center for Neuroscience
School of Medicine, Graduate School of Public Health, and the University of Pittsburgh Cancer Institute
University of Pittsburgh

Robert M. Wadowsky, Sc.D.

DEVELOPMENT AND EVALUATION OF A MINOR GROOVE BINDER-TAQMAN RT-PCR ASSAY FOR THE DETECTION OF HUMAN RHINOVIRUS IN NASAL ASPIRATE SPECIMENS

Duc H. Do, M.S.

University of Pittsburgh, 2005

A one-step real-time reverse transcription PCR (RT-PCR) assay was developed for the detection of human rhinovirus (RV) in nasal aspirate (NA) specimens. A set of primers was designed to amplify a 120-base target in the 5′ non-coding region of RV RNA. The amplicon was detected using TaqMan minor groove binder (MGB) probes and ABI Prism sequence detectors. Three probes were evaluated using stock suspensions of 15 RV strains representing serotypes 1A, 2, 3, 7, 17, 21, 29, 37, 39, 40, 58, 62, 66, 72, and 87. The initial probe that was designed, Pic-4, detected 11 of the RV strains. Probe Pic-6 was designed with a degeneracy at the first 5′ nucleotide to accommodate a target-probe mismatch. Although Pic-6 improved the detection limit for some strains, detection of RVs containing multiple mismatches was unsatisfactory. Probe Pic-5 was designed with nucleotide degeneracies at three positions to account for multiple mismatches. Pic-5 detected 14 of the RVs at a lower limit of detection of 0.00001 to 0.01 50% tissue culture infectious dose ($TCID_{50}$) equivalents/PCR reaction. RV-87, recently classified as an enterovirus (EV), was not detected with any of the probes. The assay with Pic-5 detected 30±50 copies of a plasmid containing an RV-2 target sequence. The assay yielded negative results when nucleic acids from human cells, EVs, and a panel of bacteria and viruses found in the human nasopharynx were tested. The assay with Pic-4 yielded a detection limit of 1.0 $TCID_{50}$ equivalents/PCR reaction in both neat and supernatant NA specimens seeded

with RV-2. A total of 48 NA samples obtained from children with cold-like symptoms were tested by the RT-PCR assay with probe Pic-5; 8 (16.7%) of the samples were positive. In conclusion, the real-time TaqMan MGB RT-PCR assay with Pic-5 is rapid, sensitive, and specific and has the capability of detecting at least 14 serotypes of RV. The public health significance of this study is that the RT-PCR assay with Pic-5 may lead to improvements in the diagnosis and surveillance of RV infections, and to a better understanding of the ability of RV to cause serious infection in immunocompromised patients.

TABLE OF CONTENTS

ACKNOWLEDGEMENTS ix

I. INTRODUCTION 1

A. Overview of human rhinovirus biology 1

B. Epidemiology and pathogenesis of human rhinovirus infection 3

C. Methods for the detection of human rhinovirus infection 5

D. Minor groove binder (MGB) TaqMan probe technology 6

II. GOAL AND SPECIFIC AIMS 9

A. Specific Aim 1: To develop an RT-PCR assay for the detection of RV 9

B. Specific Aim 2: To evaluate the real-time RT-PCR for detection of RV in NA specimens 11

III. MATERIALS AND METHODS 13

A. Virus strains and cultivation. 13

B. $TCID_{50}$ titer determination. 14

C. Nasal aspirate clinical specimens. 15

D. Viral RNA extraction. 15

E. Evaluation of NA materials for the detection of RV by RT-PCR. 16

F. Evaluation of purified RNA derived from NA specimens for inhibition of RT-PCR. 16

G. Nucleic acids for specificity testing. 17

H. Primers and probes. 17

I. RT and real-time PCR. 18

J. Plasmid preparation....19
K. Data analysis. 20
IV. BACKGROUND STUDIES 21
V. RESULTS 23
A. Development and optimization of the RT-PCR assay for detection of human RV 23
1. Selection of primers and MGB probes for RV detection by real-time RT-PCR ...23
2. Probe Pic-5 demonstrates optimum analytical sensitivity for detection of RV 24
3. Sensitivity analysis of the RV RT-PCR assay using a plasmid construct 35
4. The RT-PCR assay using the Pic-4 and Pic-5 MGB probes is specific for RVs...37
5. RT-PCR measurements are comparable on the ABI Prism 7700 and 7000 sequence detection systems....38
B. Real-time RT-PCR detection of human RV in nasal aspirate (NA) specimens.....39
1. Determination of RV detection limits in neat and supernatant NA samples 39
2. Determination of the RV positivity rate in young school-aged children with upper respiratory tract infection symptoms 40
VI. DISCUSSION 42
VII. FUTURE PERSPECTIVES AND PUBLIC HEALTH SIGNIFICANCE 51
APPENDIX A: Tables 54
APPENDIX B 62
Analytical comparison of the sensitivity of RV detection by RT-PCR and cell culture 62
APPENDIX C 64
RV serotypes and isolates potentially detected by the Pic-5 MGB probe as of July 2005.....64
BIBLIOGRAPHY 67

LIST OF TABLES

Table 1. Description of picornavirus strains and stock suspensions used in this study 54

Table 2. Nucleotide sequences of primers and probes used in this study 55

Table 3. Sequences of the 15 RV strains and 3 MGB probes used in this study 56

Table 4. Comparison of the detection limits of 15 serotypes of RV 57

Table 5. Detection limits for the RV plasmid and corresponding assay efficiencies 58

Table 6. Results from testing 9 EV strains by RT-PCR assays for RV and EV 58

Table 7. Results from testing heterologous DNAs and RNAs by real-time assays 59

Table 8. Comparison of RT-PCR C_T values measured on the ABI Prism 7000 and 7700 Sequence Detection Systems for RV serotype 2 60

Table 9. Comparison of RT-PCR C_T values measured on the ABI Prism 7000 and 7700 Sequence Detection Systems for RV serotype 39 60

Table 10. Comparison of RT-PCR assay measurements from testing materials derived from a pool of NA specimens seeded with varying concentrations of RV serotype 2 61

Table 11. Comparison of RT-PCR assay measurements from materials derived from a pool of NA specimens containing natural RV 61

LIST OF FIGURES

Figure 1. Schematic representation of the rhinovirus genome. 2

Figure 2. Three-dimensional structure of the rhinovirus virion. 3

Figure 3. Structure of the MGB ligand $CDPI_3$. 7

Figure 4. ΔR_n measurements by 3 probes for RV-1A, RV-2, and RVs not detected by the Pic-4 probe. 28

Figure 5. ΔR_n measurements for RVs with either no mismatches or suspected of having no mismatches with the Pic-4 MGB probe. 29

Figure 6. ΔR_n measurements for RVs with either at least 1 mismatch or suspected of having at least 1 mismatch with the Pic-4 MGB probe. 30

Figure 7. RT-PCR amplification plots for RV-66 RNA using (A) Pic-5 and (B) Pic-6 MGB probes. 31

Figure 8. C_T measurements by 3 probes for RV-1A, RV-2, and RVs not detected by Pic-4. 32

Figure 9. C_T measurements for RVs with either no mismatches or suspected of having no mismatches with the Pic-4 MGB probe. 33

Figure 10. C_T measurements for RVs with either at least 1 mismatch or suspected of having at least 1 mismatch with the Pic-4 MGB probe. 34

Figure 11. Detection of a plasmid containing the RV-2 target sequence by agarose gel electrophoresis. 35

ACKNOWLEDGEMENTS

There are a number of exceptional individuals who have had a hand in helping me reach this point in my academic life. The support during my time here in graduate school came in either fantastically colossal proportions or unbelievably minuscule notches, but every amount is appreciated all the same. I would like to thank my graduate advisor Dr. Robert Wadowsky for all of his guidance and generous advice through the last 1½ years at Children's Hospital of Pittsburgh. Dr. Wadowsky has continually encouraged me to think with a systematic mindset and to pursue scientific excellence no matter where the discipline leads me. Never will I forget that the word "lab" is jargon that is simply unacceptable for utterance in the scientific community. I would also like to thank my committee members, Drs. Lee Harrison and Frank Jenkins, for their indispensable participation and insight into this research project.

Much gratitude goes to Stella Laus and Ken Walkosak, of the Pediatric Molecular Microbiology Laboratory, for technical assistance. Thanks also to fellow student Ryan Dare for providing valuable human metapneumovirus RNA for this project, and to the entire faculty, staff, and students at IDM who I've come to know and from whom I've learned a bit of knowledge from. I wish you all the best. Thanks also to John Wheeler for the kind use of his PC notebook.

I would like to thank my friends and family for their encouragement as well through the years. Special appreciation goes to my family which has always supported and believed in me. Mom, Dad, Minh, Nam, and last but certainly not least, Hai…I love you all, and thank you.

Finally, I want to thank my fellow student, best friend, and all-around wonderful fiancée, Elizabeth Dale Ann Wheeler, whose love and support kept me going forward through good times and bad. Thanks for your patience and understanding, Elizabeth, and thank you for embarking on this remarkable journey with me. You are truly an inspiration, and I love you very much.

I. INTRODUCTION

A. Overview of human rhinovirus biology

Human rhinoviruses (RVs) are small, single-stranded RNA viruses belonging to the family *Picornaviridae*, which includes closely related enteroviruses (EVs) such as poliovirus. The viral genome consists of a positive-sense RNA of approximately 7.2 kb in size with a single open reading frame (Figure 1). Like all picornaviruses, the RV genome begins with a short peptide (VPg) bound covalently to the 5' non-coding region (5'-NCR), followed by three regions (P1, P2, and P3) that code for capsid and non-structural proteins, ending with a short 3'-NCR and a poly-A tail (48). Viral replication and protein synthesis occur in the host cell cytosol, where the genome is first translated into a large polyprotein. Several cleavage reactions mediated by virus-specific proteases generate mature viral proteins, including the structural proteins VP1-4, the site-specific proteases 2A and 3C, the RNA-dependent RNA polymerase (3D), RNA replication-associated proteins (2B, 2C, 3A), and the small protein VPg (3B) (41). The viral genome itself is subsequently copied into complementary negative-sense RNA strands that serve as templates for the synthesis of a vast number of copies of the viral genome, and these can act either as messenger RNAs for further viral protein synthesis, or can be incorporated as genomic RNA into progeny virions.

RVs are among the most rudimentary infectious agents (41). The virion is composed of a non-enveloped capsid encasing the positive-sense RNA genome. The capsid itself consists of 60 identical subunits arranged into 12 pentamers of a symmetric icosahedron, with each subunit containing one molecule each of viral proteins 1, 2, 3, and 4 (VP1-VP4). VP1, VP2, and VP3

assemble on the exterior of the virion to form a protein shell, while VP4 is attached to the interior of the capsid and interacts with the viral RNA (Figure 2). A 20-Å-deep depression, or "canyon," surrounds every five-fold axis of symmetry of the icosahedron and is found in all RV structures determined to date (6).

RVs are the most numerous of the picornaviruses, with over 100 serotypes identified (20). They are divided into major (90% of serotypes) and minor (10%) groups according to their cellular receptor usage: members of the major group bind to the intracellular adhesion molecule 1 (ICAM-1), while members of the minor group bind specifically to the low-density lipoprotein receptor family (LDLR). Interestingly, human rhinovirus serotype 87 (RV-87) was found to bind neither receptor, but to an unidentified sialic acid residue (45). Binding to cellular receptors is thought to occur by a mechanism known as the *canyon hypothesis*, in which the receptor binding sites are "hidden" inside the canyons encircling the five-fold axis to escape the neutralizing effect of bulkier antibodies (46). Evidence produced (11) demonstrated the amino acid sequences at the base of the canyon are highly conserved, while the edges of the canyon and the most extended segments of the capsid are hypervariable among the serotypes and correspond to sites of antibody neutralization (47).

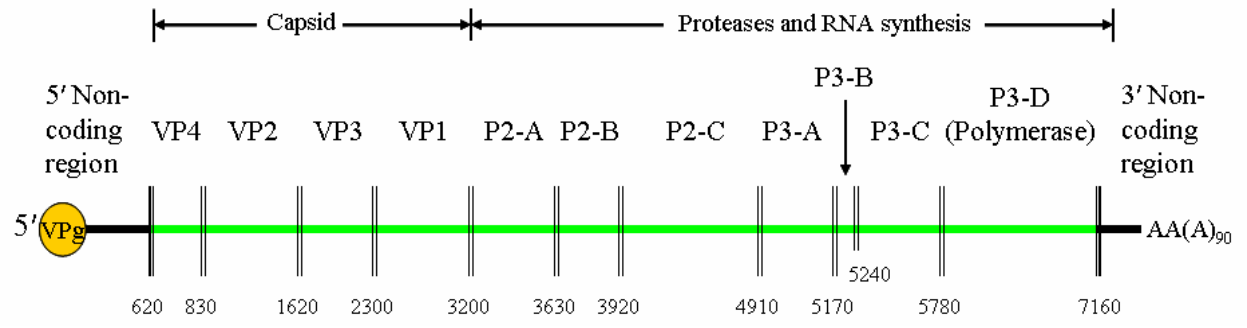

Figure 1. Schematic representation of the rhinovirus genome.

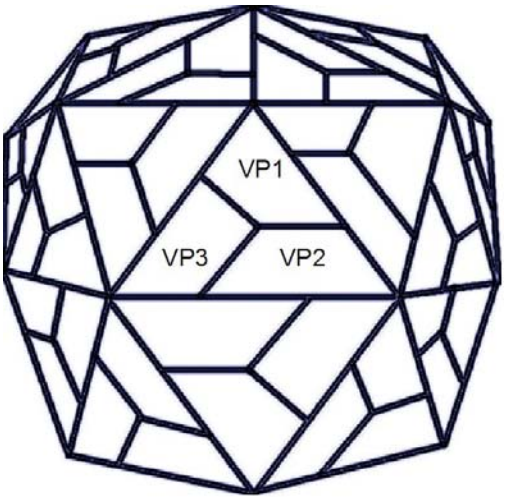

Figure 2. Three-dimensional structure of the rhinovirus virion.

B. Epidemiology and pathogenesis of human rhinovirus infection

Human RVs are well recognized as the most frequent cause of mild upper respiratory tract infection (URTI), otherwise known as the common cold. It has been estimated that RV infection accounts for 60% of cases of the common cold in adults (41), and between 10-25% of cases in children (6). As much as 80% or more of common colds are caused by RVs during the peak autumn period (21). However, for unknown reasons, not all infections result in clinical illness, with only 75% of infections leading to symptomatic colds (22). There is clear seasonality to common cold occurrences, with the frequency of respiratory infections rising sharply in the autumn, remaining high through the winter, and decreasing in the spring. A recent review article analyzing studies of rhinoviral seasonality from 1965 to 2002 confirmed the prevalence of RVs

in the autumn season (38). Despite the predominance of RV during the cold season, there is no clear prevalence of any one serotype in a given period, which seems to vary among geographical areas and over the course of time (20).

RVs are also increasingly found to be associated with more severe diseases such as sinusitis in adults, pneumonia, asthma exacerbation and otitis media in children, and more recently implicated in severe lower respiratory tract illnesses in the elderly and in immunocompromised transplant recipients (21, 27, 48, 57). Although the majority of RV infections are usually mild and self-limiting in most healthy individuals, the economic burden and contribution to overall morbidity worldwide is quite substantial (41).

Transmission of RV most commonly occurs through the respiratory-salivary route, by either hand-to-nose or hand-to-eye contact (41, 58). Small and large-particle aerosols, either lingering in the air or from a direct hit, have also been documented as another means of transmission (20). The primary site of infection is the nasal epithelium, which is also the site of viral replication (41). Upon entry into epithelial cells, virus replication begins rapidly within 6 to 8 h, with as much as 100,000 progeny virions produced per cell (7).

Pathogenesis due to RV infection is not caused directly by viral cytopathic effect, but by the release of inflammatory mediators triggered by initial infection and the release of progeny virions (18). The idea of an immune rather than a cytopathic basis of rhinoviral symptomology is supported by the fact that minimal destruction of the nasal epithelium is observed during illness (22). There is evidence that infection causes the release of a cascade of inflammatory cytokines, such as kinins, leukotrienes, histamine, interleukins-1, 6, and 8, tumor necrosis factor, and RANTES (58). RV infection of the nasal mucosa also leads to vasodilation and vascular leakage, resulting in nasal blockage and stimulation of the sneeze and cough reflexes (41). All of these

factors may contribute to the universally-known symptoms of the common cold, which include nasal stuffiness and discharge, sneezing, scratchy throat, sore throat, and cough (18, 22), although the pathogenesis of RV infection has yet to be fully understood (58). The disease course is generally self-limiting, with symptoms developing after a 24 to 48 h incubation period, peaking at 2 to 3 days after incubation, and lasting between 5 and 7 days (41).

C. Methods for the detection of human rhinovirus infection

There are several methods by which RV infection can be diagnosed and identified. The current "gold standard" of RV detection within a clinical setting is virus isolation in cell culture, followed by acid-lability testing to distinguish between RVs and EVs (48). However, virus isolation in culture is laborious and very time-consuming, often taking days or weeks for a conclusive diagnosis (9, 26, 29, 39, 50). Furthermore, some RV strains grow poorly or not at all in cell culture (30).

Serological techniques can detect neutralizing antibodies against RV and can be done in parallel with any cell culture system (41). For antibody quantification, serum titers from pre- and post-infection are compared once the serotype is known. However, due to the extensive number of serotypes (>100), serological methods are impractical and of limited value in a clinical setting.

Molecular methods are becoming more widely applied for the identification of infectious agents, including RV. With the advent of the polymerase chain reaction (PCR) technique, the field of molecular diagnostics promises faster and more reliable technologies for nucleic acid detection. Several reverse transcription-PCR (RT-PCR) assays described to date have

successfully utilized primers and probes that target the 5'-NCR of the RV genome (3, 5, 8-10, 19, 25, 43, 50), the most conserved region among human picornaviruses. RV detection has been further improved with the use of real-time TaqMan® RT-PCR, which does not require post-PCR handling and therefore reduces the risk of contamination (13, 14, 39).

There is a potential limitation of using the standard TaqMan RT-PCR assays for the detection of RVs. TaqMan probes require a melting temperature (T_m) that is at least 10ºC higher than the T_m of the primers. This feature ensures that the probe anneals before primer extension; otherwise, the extension will block probe hybridization. To achieve the higher T_m, conventional TaqMan probes must normally be longer in length than the primers. A longer oligonucleotide sequence increases the likelihood of base pair mismatches, which in turn may result in inefficient hybridization with the target region. The longer TaqMan probes also may not anneal strongly enough to all RV target sequences because of mismatches, and may therefore result in false negative results.

One way to reduce the TaqMan probe length is with the use of a relatively new technology that conjugates a minor groove binder onto a probe, as discussed in the next section.

D. Minor groove binder (MGB) TaqMan probe technology

A minor groove binder (MGB) is a molecule with very high affinity for the minor groove of double-stranded DNA rich in A-T residues (1). The MGB is usually a synthetic, non-reactive oligopeptide such as $CDPI_3$ [1,2-dihydro-(3*H*)-pyrrolo[3,2-*e*]indole-7-carboxylate] as seen in Figure 3. Because $CDPI_3$ is isohelical to the deep and narrow groove of B-form DNA, it is able to fold into the duplex and become hyperstabilized, primarily by van der Waals forces (32).

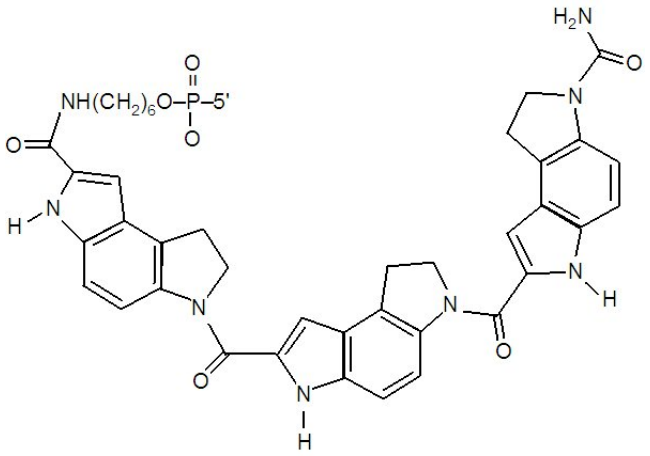

Figure 3. Structure of the MGB ligand $CDPI_3$.

TaqMan probes linked to a MGB ligand contain a fluorescent reporter molecule at the 5′ end (i.e., FAM) and a non-fluorescent quencher molecule at the 3′ end, preceded by the MGB. The synthetic MGB ligand assists the probe in annealing to the target DNA by effectively increasing the probe T_m, enabling the use of a shorter sequence (1). Additionally, TaqMan MGB probes are sensitive to single base mismatches, which increases the sequence specificity of the probe (32).

The advantages of using MGB-linked oligonucleotide probes are three-fold: (i) the MGB has high affinity for the minor groove in double-stranded DNA, allowing the probe to form extremely stable duplexes with the single-stranded DNA target; (ii) MGB probes have a higher T_m allowing for shorter, more specific probe sequences for improved hybridization of probe to target DNA and are more sensitive to single base mismatches (32, 53); and (iii) the non-fluorescent quencher molecule on the 3' end instead of the standard TAMRA™ quencher dye decreases the background fluorescence level, facilitating a higher signal-to-noise ratio (2, 32). In essence, the MGB probe is an enhancement of the TaqMan probe system.

Several recent studies have employed MGB probe technology for use in microbe detection. Ott *et al.* were able to increase the sensitivity of detection of human enteric flora 10 to 100-fold by using MGB probes targeting the conserved 16S ribosomal DNA, compared to unmodified TaqMan probes (40). Real-time PCR assays using MGB technology for the detection of human pathogens have also been evaluated for drug-resistant *Mycobacterium tuberculosis* (55), *Mycoplasma genitalium* (28), human herpes virus 7 (16), *Escherichia coli* O157:H7 (59), and more recently the severe acute respiratory syndrome–associated coronavirus (24, 35) with much success.

Using modified primers derived from published sequences (19) and custom-designed MGB probes, we applied the TaqMan MGB probe system to develop and optimize a real-time RT-PCR assay for the detection of human RV, and assessed the system using nasal aspirate (NA) clinical specimens from pediatric subjects with cold-like symptoms. Further development of this assay may allow specific and sensitive detection of nearly all 102 serotypes of RV in NA specimens. This tool will be crucial in future studies that will look at the importance of *S. pyogenes* in the common cold syndrome and the incidence of serious RV infections in immunocompromised patients.

II. GOAL AND SPECIFIC AIMS

Historically, the standard method for detection of RV has been isolation in cell culture, which until the advent of the polymerase chain reaction (PCR) made diagnosis laborious and time-consuming. Development of immunological assays to detect RV antigens is complicated by the existence of over 100 serotypes of RV (26). Recently, RT-PCR assays have been developed that detect several short conserved regions in the 5′-NCR of RV (3, 5, 8, 9, 25, 36). These assays have improved sensitivity over culture (52, 54), but there are still problems with picornavirus specificity (19, 29, 30). However, several studies in related fields have employed the use of MGB-linked oligonucleotide probes in real-time TaqMan PCR systems for the detection of several pathogens (16, 28, 34, 35, 40, 59, 60). These MGB probes enhance both the sensitivity and specificity of target detection over other detection methods (34, 40).

The goal of this research project is to develop a real-time TaqMan MGB RT-PCR assay for the detection of human RV in nasal aspirate (NA) specimens. The specific aims are described below.

A. Specific Aim 1: To develop an RT-PCR assay for the detection of RV

The objective of Specific Aim 1 is to develop and optimize a real-time MGB TaqMan RT-PCR assay to detect most, if not all, human RV serotypes. To accomplish this aim, multiple MGB probes were evaluated in RT-PCR assays by measuring the analytical sensitivity and specificity of the assays.

Aim 1a: Evaluate the detection limits for 15 strains of RV

Since it is not currently feasible to test all 102 RV serotypes in our laboratory, a panel of 15 strains of RV representing different serotypes of both major and minor groups of RV were analyzed. The lower limits of detection for these serotypes were measured in terms of $TCID_{50}$ genome equivalent units/RT-PCR reaction using 3 different TaqMan MGB probes.

Aim 1b: Assess analytical sensitivity using a plasmid DNA construct

Measuring the analytical sensitivity of the RT-PCR assay solely by testing suspensions of RV of known $TCID_{50}$ values can be misleading because the suspensions may contain viral particles that have RNA but are not infectious for the cell culture used to propagate them. One study reported that as many as 90% of the viral particles in an influenza virus suspension were noninfectious for a cell culture system (23). Therefore, the analytical sensitivity of the RT-PCR assay was assessed by developing a plasmid containing an insert of the RV-2 PCR product. The plasmid was then used to determine the lowest copy number detectable by the assay.

Aim 1c: Assess the analytical specificity of the assay

Much of the 5′ NCR sequences of picornaviruses are shared by both RVs and EVs. To demonstrate that our assay is specific for RVs, the detection of 9 different strains of EVs by real-time RT-PCR was evaluated. Furthermore, it must be demonstrated that the assay does not detect nucleic acids from human DNA, from other common viruses, or from bacteria found in the human nasopharynx.

Aim 1d: Evaluate assay measurements on the ABI Prism 7000 and 7700 Sequence Detection Systems.

There are two ABI Prism sequence detection systems available in the Pediatric Molecular Microbiology Laboratory at Children's Hospital of Pittsburgh: the 7700 model, and the newer 7000 model. The instruments were evaluated for providing comparable results.

B. Specific Aim 2: To evaluate the real-time RT-PCR for detection of RV in NA specimens

The objective of Specific Aim 2 is to evaluate the RT-PCR assay for detection of RV in NA specimens. To address this objective, it was necessary to determine the detection limit of RV in NA specimens, assess the frequency of RV in a human population, and evaluate inhibition of the RT-PCR assay by purified nucleic acids isolated from NA specimens.

Aim 2a: Determine the detection limits for RV in NA specimens.

The manufacturer's instructions included in the QIAamp® Viral RNA Mini Kit indicate that only cell-free body fluids can be used for preparation of viral RNA. Since NA specimens may contain human cells and mucous harboring RV, a comparison of RV detection in both neat (whole) and supernatant (cell-free) NA specimens was performed. This comparison addressed whether neat or supernatant NA had any impact on viral RNA purification and determined whether nucleic acids isolated from the NA specimens by the QIAamp kit would interfere with RT-PCR.

Aim 2b: Assess the frequency of RV infection in school-aged children with upper respiratory tract symptoms.

A study was conducted to assess the frequency of RV infection in a group of pediatric subjects with cold-like symptoms who were enrolled in a Group A *Streptococcus* study at the Falk School, University of Pittsburgh. NA specimens collected from these subjects were tested by the RT-PCR assay to determine if RV was present. In addition, the rate of RT-PCR inhibition by nucleic acids isolated from these NA specimens was determined.

III. MATERIALS AND METHODS

A. Virus strains and cultivation.

Strains of rhinoviruses (RVs) and enteroviruses (EVs) (Table 1) were obtained from the American Type Culture Collection (ATCC; Manassas, VA). RVs were propagated using WI-38 human embryonic lung fibroblast cell culture tubes (16 x 125 mm), and EVs were propagated using rhesus monkey kidney cell culture tubes (16 x 125 mm). The cell culture tubes were obtained generally near confluency from Viromed Laboratories (Minnetonka, MN) and were examined upon arrival for cytopathic effect (CPE) or other abnormalities. Stock suspensions of virus obtained from the ATCC were diluted 10^{-1} and 10^{-2} in Eagles-Minimum Essential medium containing 2% heat-inactivated fetal bovine serum, 100 units/ml penicillin, 10 μg/ml gentamicin, 2.5 μg/ml Fungizone, and 20 mM Hepes buffer (Viromed Laboratories). After removing the medium from cell culture tubes, 0.2-ml portions each of the undiluted suspension and the dilutions were inoculated onto duplicate cell culture monolayers. Control monolayers were inoculated with 0.2 ml of medium. All tubes were then incubated in a stationary position at either 33°C for RV propagation or at 37°C for EV propagation for 1 h to allow for virus adsorption. After incubation, 1 ml of pre-warmed medium (i.e., at 33°C and 37°C for RV and EV propagation, respectively) was added to each tube. The tubes used for RV propagation were further incubated on a roller drum (0.5-0.75 rpm) to enhance infection of the cells by RV, while tubes used for EV propagation were incubated stationary at 37°C. Inoculated cell culture tubes were incubated for 7-10 days and were examined microscopically for the progression of CPE periodically between days 2 and 7. Final CPE readings were taken between days 7 and 10, depending on when maximal CPE was observed. CPE was rated according to the following

scale: 0, no CPE; 1+, <25% CPE; 2+, 25-49% CPE; 3+, 50-74% CPE; and 4+, 75-100% CPE. A tube was scored as positive for virus growth only if the CPE was greater than 1+ since un-inoculated control tubes occasionally showed small degrees of CPE-like changes, generally less than 5% of the cell monolayer. Virus was harvested from the cell cultures showing 3 to 4+ CPE by first subjecting the cell culture tubes to three consecutive freeze-thaw cycles (i.e., -80°C and room temperature). The culture tubes were then centrifuged for 15 min at room temperature at 3,000 rpm using a Beckman GS-6R centrifuge equipped with a GH-3.8 rotor (Beckman Coulter; Fullerton, CA). Supernatants were collected and aliquoted into 0.2-ml portions, which were stored at -80°C.

B. $TCID_{50}$ titer determination.

The concentration of RV in a stock suspension was determined by measuring the 50% tissue culture infectious dose ($TCID_{50}$) titer. Aliquots of the stock suspension were removed from storage at -80°C, quickly thawed in a 37°C water bath, and serially diluted in ten-fold steps in the 2% Eagles-Minimum Essential medium. Medium was removed from WI-38 cell culture tubes, followed by the addition of 0.1 ml-portions from each virus dilution (10^{-2}-10^{-6}) in six replicate tubes. As controls, two tubes were inoculated with 0.1 ml of the cell culture medium. The inoculum was allowed to adsorb onto the cell-culture monolayers for 1 h at 33°C, the temperature of the human nasal passage. Subsequently, 1 ml of the cell culture medium was added to each tube. The tubes were then incubated for 7-10 days on a roller drum and were periodically examined for CPE during this period. Final CPE readings were determined between days 7-10 as described above. $TCID_{50}$ titers were calculated using the method of Reed-Muench (44), and determinations were done in duplicate for each RV strain (Table 1).

C. Nasal aspirate clinical specimens.

Nasal aspirate (NA) specimens (n = 48) were obtained from subjects enrolled in a Group A Streptococcal study conducted at the Falk School, University of Pittsburgh. In this substudy, subjects were evaluated between October 2002 and February 2003 when they had symptoms consistent with an upper respiratory tract infection. At the evaluation, a nasal aspirate specimen was obtained by suction. Occasionally, the nasal aspirate material became lodged in the catheter tubing. In these instances, the specimen material was dislodged from the catheter tubing by rinsing it with one to two ml of sterile saline. To prevent degradation of viral particles, bovine serum albumin was added to the NA specimens at a final concentration of 0.025% (wt./vol.). The specimen suspension was then aliquoted into 0.3-ml volumes and stored at -80°C. Negative controls for the testing of NA specimens in the RT-PCR assay were prepared by adding bovine serum albumin to diethylpyrocarbonate-treated water (DEPC-H_2O) (Ambion; Austin, TX) at a final concentration of 0.025% (wt./vol.). These controls were stored in 0.2-ml aliquots at -20°C.

D. Viral RNA extraction.

RV RNA was extracted from samples using the QIAamp® Viral RNA Mini Kit (Qiagen; Valencia, CA) according to manufacturer's instructions. Briefly, 140 µl of samples (i.e., NA specimens, virus stock suspension dilutions, and control samples) were added to a lysis buffer. RNA from the lysates was captured on a silica spin column and eluted in a final volume of 60 µl of an elution buffer. For determination of the lower limit of detection by RT-PCR, the purified viral RNA was serially diluted in ten-fold steps in DEPC-H_2O containing 30 µg/ml yeast tRNA (Ambion; Austin, TX). The yeast tRNA acts as a co-precipitant and aids in the quantitative recovery of small amounts of nucleic acids in dilute solutions.

E. Evaluation of NA materials for the detection of RV by RT-PCR.

Whole (neat) and cell-free (supernatant) NA materials were evaluated for the detection of RV by the RT-PCR assay using seeded samples. In the first experiment, aliquots from 7 NA specimens were removed from storage at -80°C and quickly thawed in a 37ºC water bath, and combined into a pool. An aliquot of a RV-2 stock suspension was prepared similarly and then diluted in the pooled specimens (i.e., 4 µl of sample to 396 µl of pooled NA material in 1.5-ml microcentrifuge tubes) to provide samples containing 1, 10, 100, and 1,000 $TCID_{50}$ equivalent genome units/ml. A 140-µl volume of the neat material was removed from each sample. The remaining sample volumes were centrifuged in an Eppendorf 5417R microcentrifuge equipped with a FA 45-30-11 rotor (Eppendorf North America; Westbury, NY) at 14,000 rpm for 5 min at room temperature. A 140-µl volume of supernatant was removed from each sample. RNA was isolated from 140-µl volumes of the neat and supernatant samples by the QIAamp procedure. In the second experiment, the pool of NA specimens was prepared from 17 aliquots, all from separate specimens. Testing of this pool by RT-PCR demonstrated that it contained RV. Therefore, it was not necessary to seed this pool with a stock suspension of RV to conduct this experiment. Otherwise, the conditions were the same as in the first experiment.

F. Evaluation of purified RNA derived from NA specimens for inhibition of RT-PCR.

Volumes (5 µl) of the RNA samples isolated from 48 NA specimens by the QIAamp Viral RNA kit were tested in duplicate RT-PCR reaction mixtures containing 10,000 genome equivalent units of RV-2 RNA. Testing of DEPC-H_2O (5 µl/reaction) served as a control for inhibition. These samples were tested by the RT-PCR assay with Pic-5.

G. Nucleic acids for specificity testing.

Purified DNA and RNA from various respiratory viruses and bacteria that are found in the human nasopharynx were obtained from a collection maintained in the Pediatric Molecular Microbiology Laboratory (Children's Hospital of Pittsburgh, PA). Purified RNA from human metapneumovirus was obtained from the Clinical Virology Laboratory at the University of Pittsburgh Medical Center Presbyterian Hospital.

H. Primers and probes.

Forward primer Pic-1 and reverse primer Pic-3 (Table 2) were designed by the Primer Express version 1.5 software program (Applied Biosystems; Foster City, CA) to amplify a 120-base RNA target in the 5′-NCR of RV. Pic-1 and Pic-3 have melting temperatures (T_m) of 59.9 and 58.1ºC, respectively.

The TaqMan MGB probe Pic-4 (T_m = 68.8ºC) was designed with Primer Express by analyzing the region between the Pic-1 and Pic-3 primer annealing sites for RV strain 9503031 (GenBank accession no. AF108174) (3). The nucleotide sequence of the six conserved subregions in the NCR of this strain is nearly identical to a RV consensus sequence (3). Two modifications of Pic-4, designated as Pic-5 and Pic-6, were subsequently designed with nucleotide degeneracies in an attempt to increase the number of RV serotypes detected by the assay (Table 2). The 16-nucleotide MGB probes were synthesized with the reporter dye FAM on the 5' end, and a minor groove binder followed by a non-fluorescent quencher on the 3' end. A BLAST search with these probe sequences yielded no perfect-match hits with EVs, other viruses (except RV), and bacteria common in the human respiratory tract. Primers and probes for the EV RT-PCR assay and eubacterial 16S rRNA PCR assay were described previously (12, 37).

I. RT and real-time PCR.

RT was performed using MultiScribe™ reverse transcriptase included in the TaqMan® One-Step RT-PCR Master Mix Reagents kit (Applied Biosystems; Foster City, CA). The final reaction mixture contained 5 µl of purified RNA, 25 µl of 2X Universal PCR Master Mix, 1.25 µl of 40X MultiScribe™ and RNase Inhibitor Mix, 900 nM (each) of primers Pic-1 and Pic-3, and 150 nM of MGB probe to a final volume of 50 µl per reaction. Reactions were performed in duplicate. RT-PCR was carried out using either an ABI Prism 7000 sequence detection system or an ABI Prism 7700 sequence detection system (Applied Biosystems; Foster City, CA). Except for comparative studies performed with the two instruments, all other experiments were conducted using the ABI Prism 7000. The RT step was performed for 30 min at 48ºC, then immediately followed by real-time TaqMan PCR under the following conditions: 10 min at 95ºC, 45 cycles of 15 s at 95ºC and 1 min at 60ºC. Data are reported in two types of measurements, the cycle threshold (C_T) value and the ΔR_n value. The C_T value is defined as the fractional PCR cycle number at which amplification is first detected; thus, a low C_T value results from a high input copy number of RV RNA. By definition, a negative result is assigned a C_T value of 45, the number of cycles conducted. Samples were considered positive for amplicon production when the C_T values were less than 45 and the amplification plot clearly demonstrated exponential increase in reporter signal in duplicate PCR reactions. Samples that had only a single positive replicate were considered as indeterminant and required repeat testing. The ΔR_n value is a measure of the normalized fluorescent reporter signal generated during the PCR amplification; as more probe binds specifically to the target, more fluorescence is produced from cleavage of the probe during the extension/polymerization phase of PCR. A negative PCR result generally corresponds to ΔR_n values close to 0, while strong amplification corresponds to ΔR_n values of about 3.0.

For comparing C_T measurements between the ABI Prism 7700 and 7000 instruments, stock suspensions of RV-2 ($TCID_{50}$ unknown) and RV-39 were tested in the RT-PCR assay by serially diluting the purified RNAs in 10-fold steps in DEPC-H_2O. Duplicate 50-µl aliquots of each of these reaction mixtures were then loaded into two 96-well plates. One plate was placed into a ABI 7000 Sequence Detector and the other plate was placed into a ABI 7700 Sequence Detector for RT-PCR amplification and detection.

The real-time PCR detection of EVs and eubacteria was performed as above, except using EV-specific and eubacterial 16S rRNA-specific primers and probes (Table 2).

J. Plasmid preparation.

A DNA plasmid was constructed by cloning the 120-base RV-2 cDNA RT-PCR product into a pCR®2.1-TOPO plasmid vector using the TOPO TA Cloning® Kit (Invitrogen; Carlsbad, CA) following manufacturer's instructions. A 72°C extension step was required after the initial RT-PCR cycling conditions in order to produce the adenosine (A) overhangs in the PCR amplicon for proper ligation into the vector containing the thymidine (T) overhangs. Successful *E. coli* transformants were subcultured, and plasmid was purified from these transformants using the QIAprep® Spin Miniprep Kit (Qiagen; Valencia, CA) according to manufacturer's protocol. Plasmid products were loaded onto a 1% agarose gel containing 0.5 µg/ml ethidium bromide and were separated by electrophoresis at 80 V/cm for 3 to 5 h. Bands were visualized on a Fotodyne UV 21 Transilluminator (Hartland, WI) and captured by a Fotodyne FCR-10 polaroid camera. Gel-purification of plasmid was performed using the QIAquick® Gel Extraction kit (Qiagen; Valencia, CA) following manufacturer's instructions.

The DNA concentration of the plasmid was determined by spectrophotometric measurement using a Beckman DU 640 spectrophotometer (Beckman Coulter; Fullerton, CA), and the number of plasmid copies in the extract was calculated from the molecular weight of the vector and the insert. Plasmid was stored at -20°C until use.

K. Data analysis.

To calculate the efficiency of the RT-PCR assay, the following equation was used: $E = (10^{1/-m} - 1) \times 100$, where E is the efficiency and *m* is the slope of the standard curve. Differences in the means of C_T values between neat and supernatant NA samples were analyzed by the student *t*-test.

Statistical analysis of the means of the CT values for RVs among the three MGB probes (Figures 8 to 10) was performed by comparing the confidence intervals obtained

For the analytical comparison of the detection limits of RV between RT-PCR and cell culture (Appendix B), the following equation was used to calculate the initial concentration of RV RNA in a starting material: $C_i = X((60/140)/.005)$, where C_i is the initial concentration (expressed as $TCID_{50}$ genome equivalents/ml), X = detection limit by RT-PCR ($TCID_{50}$ genome equivalents/PCR reaction), 60/140 is the dilution factor of the QIAamp purification process, and 0.005 is the volume (ml) of purified RNA added to a single RT-PCR reaction to obtain the detection limit. The C_i value was then multiplied by 0.2 (ml), the volume of a viral stock suspension that would be inoculated onto a cell culture tube. The resulting value is the calculated number of $TCID_{50}$ that would give a positive result by cell culture. An expected cell culture result would be called positive if the calculated $TCID_{50}$/tube number approached a value of 1.0.

IV. BACKGROUND STUDIES

A brief description of the background work done previously for the project (performed by R. Wadowsky and S. Laus, Children's Hospital of Pittsburgh; personal communication) is described below.

Seven serotypes (2, 7, 21, 29, 37, 39, 58) were propagated in WI-38 cells (human embryonic lung fibroblasts) on a rotator at 33ºC. Stock suspensions of these serotypes were prepared and stored at -80ºC. The $TCID_{50}$ of RV-39 was determined to be $10^{-4.5}$/0.1 ml.

The Pic-1 and Pic-3 primer set was evaluated for its ability to amplify the RNA target by testing RNA purified from RV-39 in a one-step RT-PCR assay containing the fluorescent dye SYBR green, which binds to double-stranded DNA and also by evaluating the PCR products by agarose gel electrophoresis. PCR reactions that contained the RV RNA yielded a single major amplification product corresponding to the 120-base target on the basis of both dissociation curve analysis and agarose gel electrophoresis. In an optimization study, use of both primers at 900 nM to amplify RV-58 RNA appeared optimal. These results indicated that the Pic-1, Pic-3 primer pair is suitable for reverse transcription and PCR amplification of the RV target.

Seven RV strains have been tested by the RT-PCR assay at a moderate level of input (i.e., RNAs purified from a 1/100 dilution of the stock suspensions) using the Pic-4 probe. All 7 RV strains were detected in the assay. However, the C_T values for serotypes 37 and 39 tended to be higher than those from the other serotypes and correspondingly the ΔR_n values were lower. Analysis of the nucleotide sequences for the probe annealing site indicated that the serotype 37 and 39 strains have mismatches with some of the nucleotides of the probe. These results suggested that use of a mixture of MGB probes that covers the sequence variability might increase the detection limit for the 37 and 39 strains and possibly other serotypes as well.

The detection limit for the RV-39 stock ($TCID_{50}$ = $10^{-4.5}$/0.1ml) was determined to be 0.04 $TCID_{50}$ genome equivalents/PCR reaction (corresponding to a 10^{-5} dilution of the stock suspension) in duplicate TaqMan PCR reactions. The PCR product was also detected down to a 10^{-5} dilution by agarose gel electrophoresis.

To determine whether an enterovirus strain would be detected by the rhinovirus RT-PCR, a strain of Coxsackievirus serotype A9 (patient isolate at Children's Hospital of Pittsburgh, serotyping done by Allegheny County Health Department) was tested. RNA from this enterovirus was not detected in the rhinovirus RT-PCR using Pic-1 and Pic-3 primers and the Pic-4 MGB probe. A C_T value of 45 was obtained by the TaqMan assay, and no bands were observed on the agarose gel. To determine if RV RNA could be detected in an established RT-PCR assay designed for the detection of enterovirus, purified RNA from RV serotype-39 was tested and yielded a negative result.

V. RESULTS

A. Development and optimization of the RT-PCR assay for detection of human RV

1. Selection of primers and MGB probes for RV detection by real-time RT-PCR

There are 6 sub-regions (A-F) of nucleotide sequences, each approximately 20 bases in length, within the 5′ non coding region (5'-NCR) of the RV genome that are considered reasonably well conserved across different rhinovirus serotypes (3). These sub-regions are separated by nucleotide sequences that are variable among RVs (3, 14). A set of primers, Pic-1 and Pic-3, was designed to amplify a 120-base target located within sub-regions E and F. The primers were intended to be complementary to sequences in sub-regions E and F since analysis of this region indicated that its length of less than 150 bases is ideal for designing a TaqMan primer-probe set. The primer pair, using the Pic-4 MGB probe, successfully detected seven RV serotypes in preliminary studies done previously at the Pediatric Microbiology Laboratory (data not shown). However, a BLAST query within the GenBank database (at the National Center for Biotechnology Information) revealed that the Pic-1 and Pic-3 primers are not specific for RVs, with numerous sequence hits for EVs and other picornaviruses. The shared homology between RVs and EVs with the target region is in accordance with a similar set of primers previously described (19).

The initial fluorescent dye-labeled TaqMan MGB probe designed was a 16-mer oligonucleotide, designated as Pic-4 (Table 2), which anneals adjacent to primer Pic-1 with a one-base separation between the primer and probe. Binding of this oligonucleotide probe with the MGB ligand effectively increases the T_m of the probe and thereby allows the use of a shorter

sequence. Pic-4 has perfect sequence alignment with the RV target sequence (Table 3), and was able to detect 11 RV serotypes (1A, 2, 3, 7, 21, 29, 37, 39, 40, 58, and 62) (Table 4). Apparently, the Pic-4 MGB probe did not bind well or did not bind at all to RV serotypes containing mismatches, particularly at the first 5′ position of the target. Therefore, two additional MGB probes were designed with nucleotide degeneracies to accommodate three base mismatches not covered by Pic-4. Probe Pic-5 contains three degenerate nucleotides at positions 1, 10, and 11 relative to the Pic-4 sequence, and probe Pic-6 contains one degeneracy at the first position (Table 3). All three probes were evaluated for the detection of the 15 RV serotypes in the study panel. None of the probes detected members of the genus Enterovirus when a BLAST search with the MGB nucleotide sequences was performed. The overall rationale was to design MGB probes that would detect as many RV serotypes as possible, based on all deposited RV 5′ NCR sequences currently available in GenBank.

2. Probe Pic-5 demonstrates optimum analytical sensitivity for detection of RV

To determine the lower limit of detection of RV by real-time RT-PCR using the three MGB probes Pic-4, Pic-5, and Pic-6, a 10-fold dilution series of purified RV RNA was prepared for each serotype. Results of RT-PCR testing and a comparison of detection limits for each RV serotype by MGB probe are shown in Table 4.

With probe Pic-4, 11 (i.e., 1A, 2, 3, 7, 21, 29, 37, 39, 40, 58, and 62) of 15 serotypes were detected with very good sensitivity ranging from 0.1 to 0.0001 $TCID_{50}$ genome equivalent units/PCR reaction (Table 4). These results indicated that the RT-PCR assay was much more sensitive than cell culture for some strains of RV (Appendix B). However, probe Pic-4 failed to

detect serotypes 17, 66, 72, and 87 even at the highest input value of purified RNA tested (Table 4 and Figure 4). RV-17, RV-72, and RV-87 all have a T-to-C base mismatch at the first nucleotide position of the probe and one or two additional mismatches before position no. 12 (Table 3), which likely prevents the 5′ end of Pic-4 from annealing properly to its target. RV-1A and RV-37 also have the T-to-C base mismatch at the first nucleotide position and no other mismatches before position no. 14, and they were detected by Pic-4. This observation implies that at least two mismatches before position no. 12 for serotypes 17, 66, 72, and 87 were additional factors that prevented the annealing of the probe. Therefore, the probe Pic-4, based on its inability to detect 4 RV serotypes, was eliminated as a candidate for inclusion into the final RT-PCR assay.

MGB probe Pic-5 detected 14 RV serotypes (i.e., all but RV-87) with good sensitivity, including three serotypes (i.e., 17, 66, 72) that were not detected by Pic-4 (Table 4 and Figure 4). The RV-87 target sequence contains two mismatches not covered by Pic-5, at positions 8 and 16 (Table 3), likely rendering the probe ineffective for annealing to this target. Serotype 1A, which was weakly detected by probe Pic-4, displayed improved detection as evidenced by increased ΔR_n signal (Figure 4A, open circles). Detection limits for the other strains ranged from 0.01 to 0.00001 $TCID_{50}$ genome equivalent units/PCR reaction. The results from these studies indicated that Pic-5 was a good candidate for inclusion into the RT-PCR assay.

There is a potential shortcoming of the Pic-5 probe, however, in that detection of strains with no mismatches to the Pic-4 probe sequence (i.e., strains 2, 7, 21, 29, 40, 58, and 62) yielded a marked decrease in the ΔR_n signal generated compared to the signals generated with Pic-4 (Figure 5). Additionally, probe Pic-5 performed no better (Figure 6B) or even worse (Figure 6A and C) than the Pic-4 probe when detecting serotypes that had at least 1 mismatch with probe

Pic-4. It is important to note, however, that the ΔR_n signal produced by Pic-4 was much lower in the strains presented in Figure 6 than the strains with perfect matches presented in Figure 5.

In an attempt to circumvent these deficiencies, MGB probe Pic-6 was designed with the rationale that a solution of probes that cover the mismatch at position no. 1 would detect most if not all of the RV strains since the next closest mismatch in any RV strain does not occur until position no. 8, thereby facilitating a large portion of the 5′ end of the probe to anneal to the target. Furthermore, since the reporter molecule is attached to the 5′ end of the probe, it was reasoned that the nucleotide at position no. 1 was crucial for a robust production of reporter signal. Therefore, Pic-6 contained a single degeneracy at position 1 that accounted for T and C bases. Results from the RT-PCR assay with Pic-6 show that this reasoning was supported only by RV serotype 1A, which exhibited a marked increase in ΔR_n signal compared to Pic-4 and Pic-5 (Figure 4A). The prototype strain RV-2 also showed improved ΔR_n signal with Pic-6; since RV-2 has a perfect sequence match with the original Pic-4 probe, the reason for the improved ΔR_n signal with Pic-6 is unclear. RV-87 was not detected by this probe (Table 4). Serotypes 17, 66, and 72 were not detected by Pic-4, but were detected by Pic-6, although the ΔR_n signal generated with these serotypes was less than the signal produced by Pic-5 (Figure 4C, D, and E, respectively). This reduction is probably attributed to the mismatches at other positions to the probe in addition to position no. 1 in these serotypes. The decrease in reporter signal is a significant disadvantage to using Pic-6 in terms of detecting RVs with multiple mismatches, as evidenced by the RT-PCR amplification plots from RV-66 (Figure 7). RNA from RV-66, which likely contains multiple nucleotide mismatches as shown by Pic-4 testing (Figure 4D), was amplified and tested for real-time detection using the Pic-5 and Pic-6 probes. Pic-5 yielded clear, exponential amplification of serial 10-fold dilutions of the target RNA (Figure 7A), whereas Pic-

6 demonstrated notably weaker amplification (Figure 7B). Taken together, these results suggest that Pic-6 is not an ideal probe to be utilized for the detection of RV serotypes containing mismatches at positions other than at the first 5′ nucleotide position. Evaluation of Pic-6 in the RT-PCR testing of the remaining RV serotypes was discontinued and Pic-6 was eliminated from consideration for inclusion into the RT-PCR assay.

An analysis of the C_T value measurements for the RV strains tested was performed at a standardized threshold level as another means to compare probe efficacy. The threshold level is an adjustable value used to indicate the point where the amplification plot of a sample is above the baseline fluorescence. For this analysis, the threshold level was set to a value of 0.015 to measure the exponential amplification of the RV target. Comparisons of the C_T values generated by the three MGB probes among the RVs detected showed a clear advantage of probes Pic-5 and Pic-6 for RV strains not detected by probe Pic-4 (Figure 8), but neither probe was observed to be more advantageous than the other. No marked differences were seen in the C_T values among RV strains with perfect target sequence matches between the Pic-4 and Pic-5 probes (Figure 9), nor for the strains (i.e., 3, 37, and 40) with at least 1 mismatch with the Pic-4 probe sequence (Figures 10A, 10B, and 9D, respectively). Although differences between the mean C_T values produced by Pic-4 and Pic-6 in RV-1A (Figure 8A) and between Pic-4 and Pic-5 in RV-39 (Figure 10C) appear visually noteworthy, a statistical analysis of the confidence intervals of the means indicates that these differences are not significant.

From this set of experiments it was concluded that the Pic-5 probe was the best choice for inclusion into the RT-PCR assay. Although it has the disadvantage of reduced reporter signal compared to the other probes, Pic-5 was able to detect 14 of the 15 RV serotypes included in the RV challenge panel.

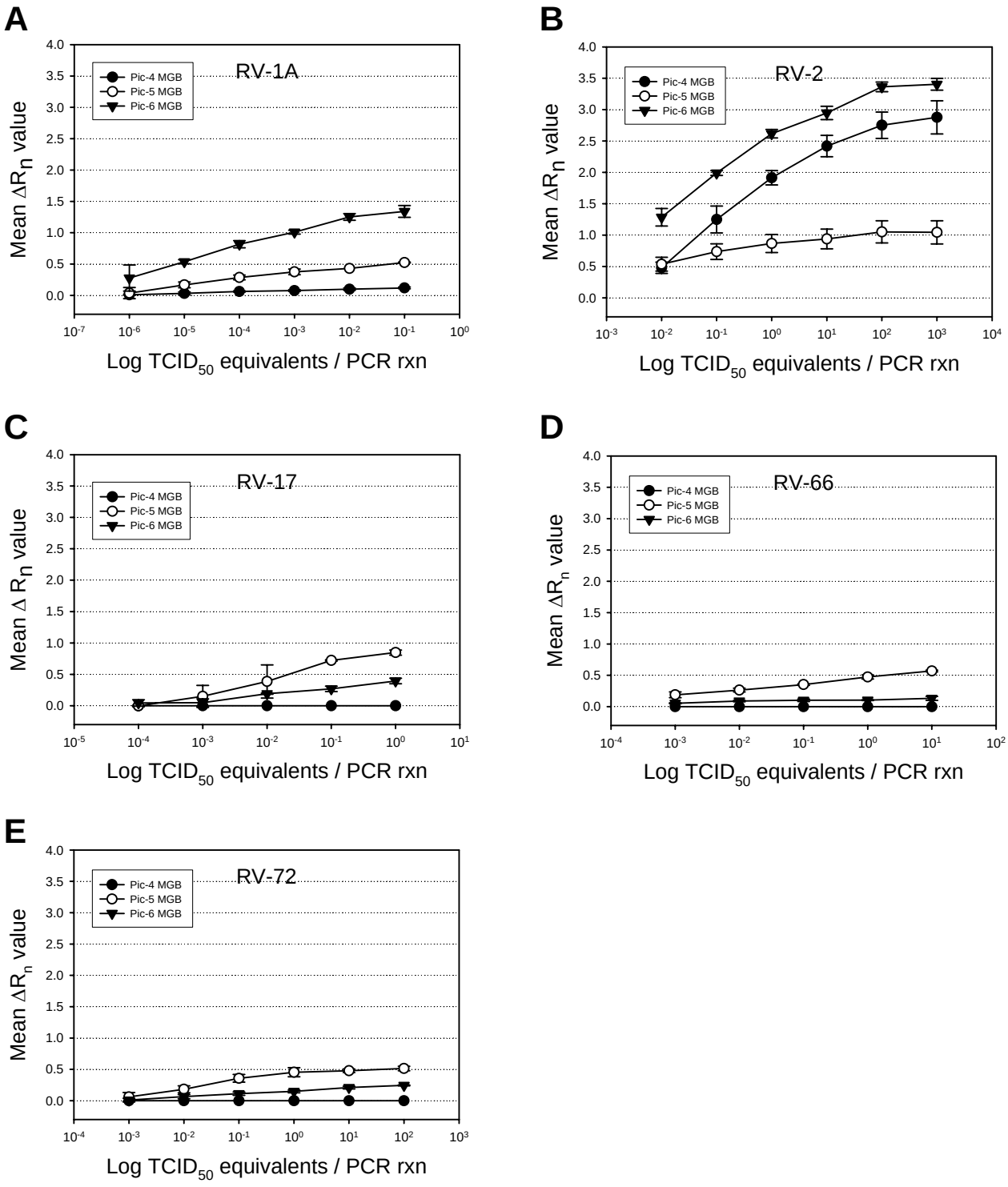

Figure 4. ΔR_n measurements by 3 probes for RV-1A, RV-2, and RVs not detected by the Pic-4 probe.

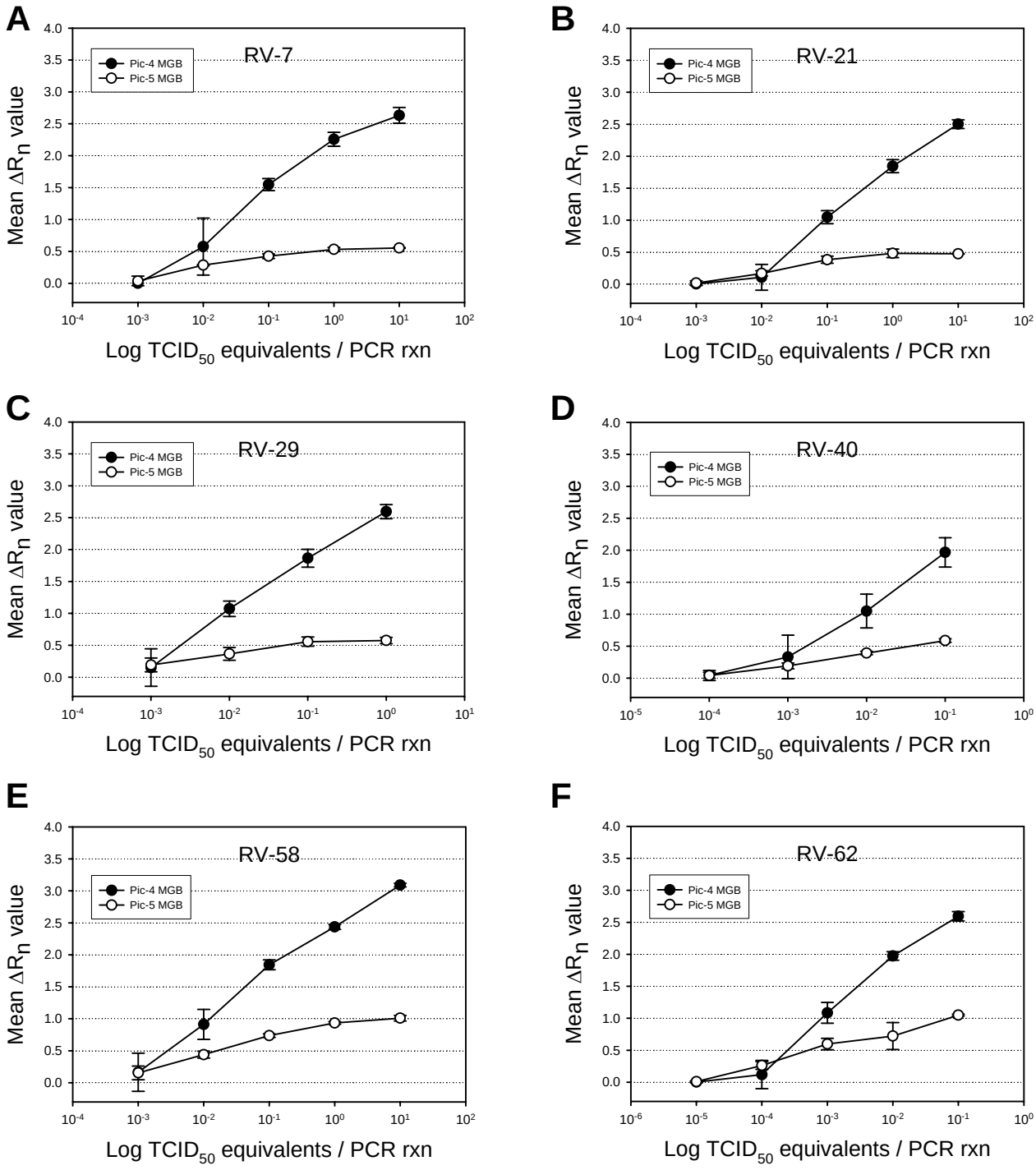

Figure 5. ΔR_n measurements for RVs with either no mismatches or suspected of having no mismatches with the Pic-4 MGB probe. Strain RV-40, which does not have target sequence information, is grouped here because of the similarity of its ΔR_n pattern to the patterns found with the strains known to have no mismatches. RV-2, which also contains no mismatches, is not included here because it was used for the 3 probe comparison study in Figure 4.

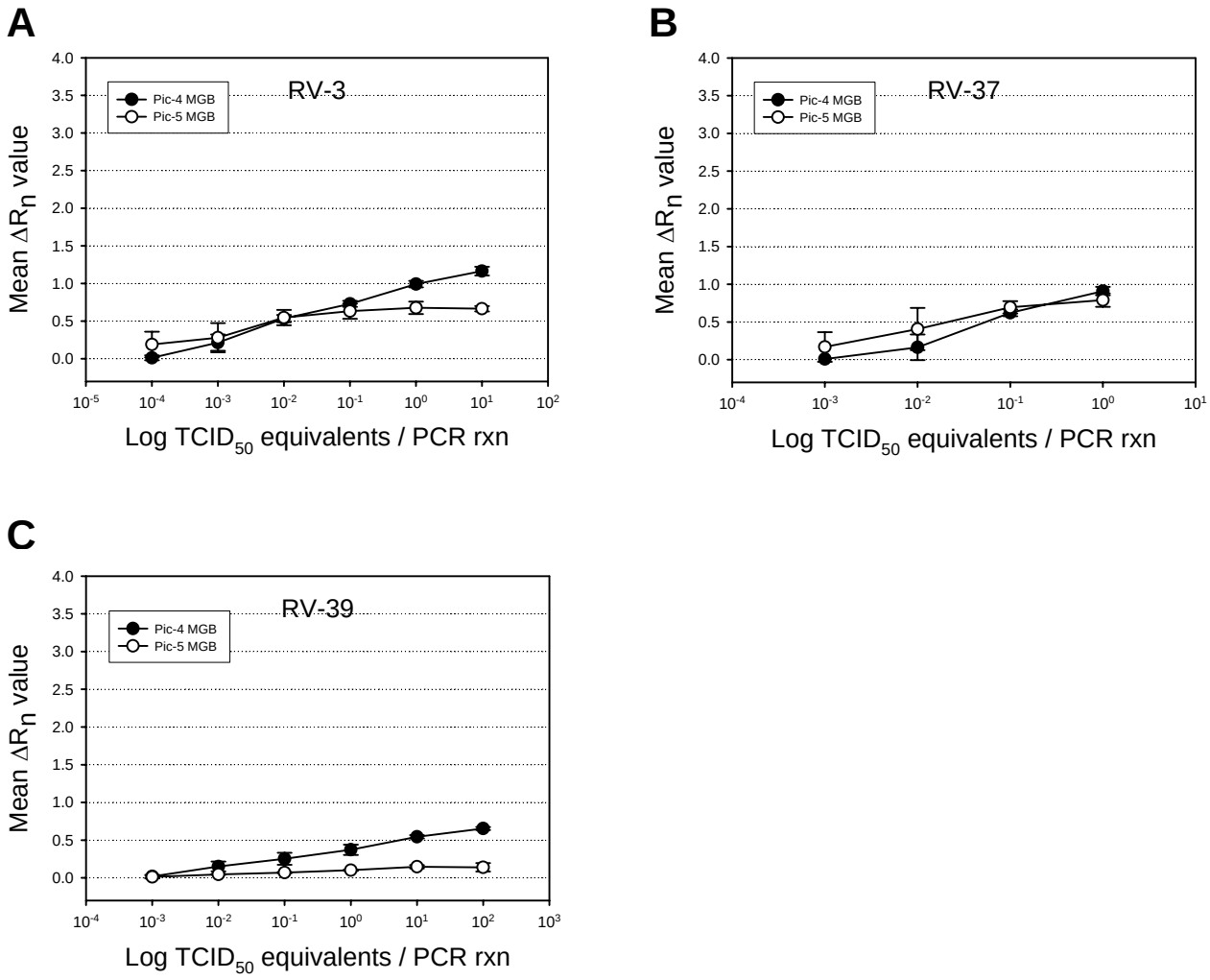

Figure 6. ΔR_n measurements for RVs with either at least 1 mismatch or suspected of having at least 1 mismatch with the Pic-4 MGB probe. Strain RV-3, which does not have sequence information, is grouped here because of the similarity of its ΔR_n pattern to the patterns found with the strains known to have 1 mismatch. RV-66, also suspected of having at least 1 mismatch with the Pic-4 probe, is not included here but in the 3 probe comparison study shown in Figure 4. Strains 1A, 17, and 72 have at least 1 known mismatch but are not shown here for the same reason as RV-66.

A

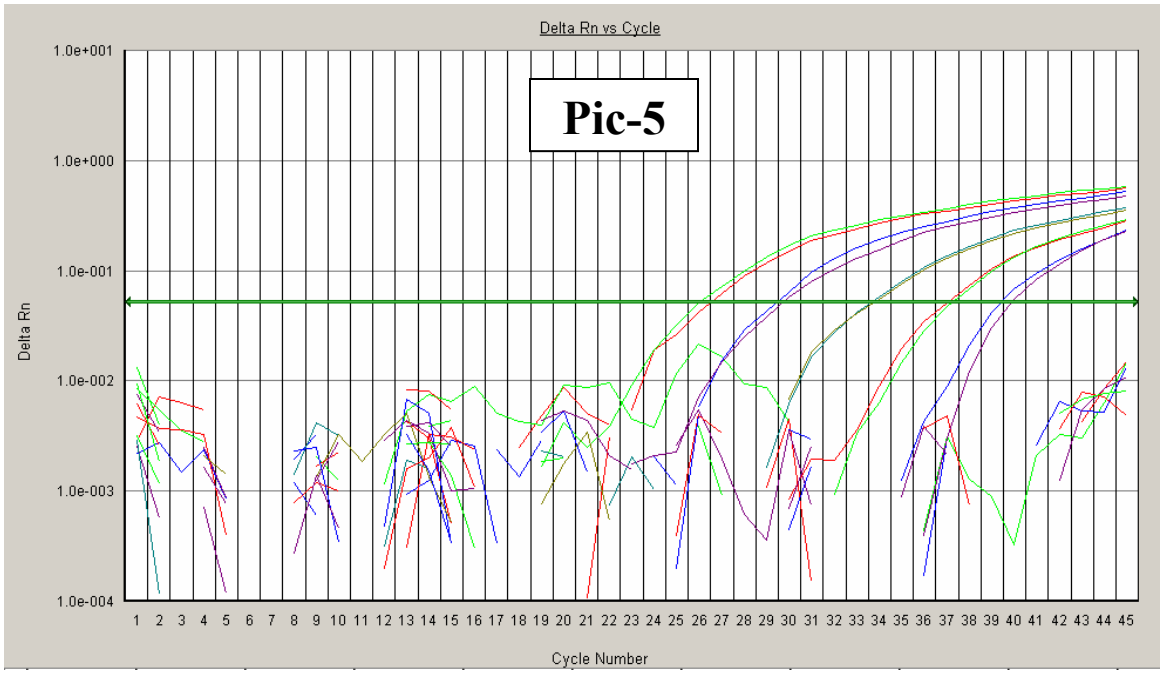

B

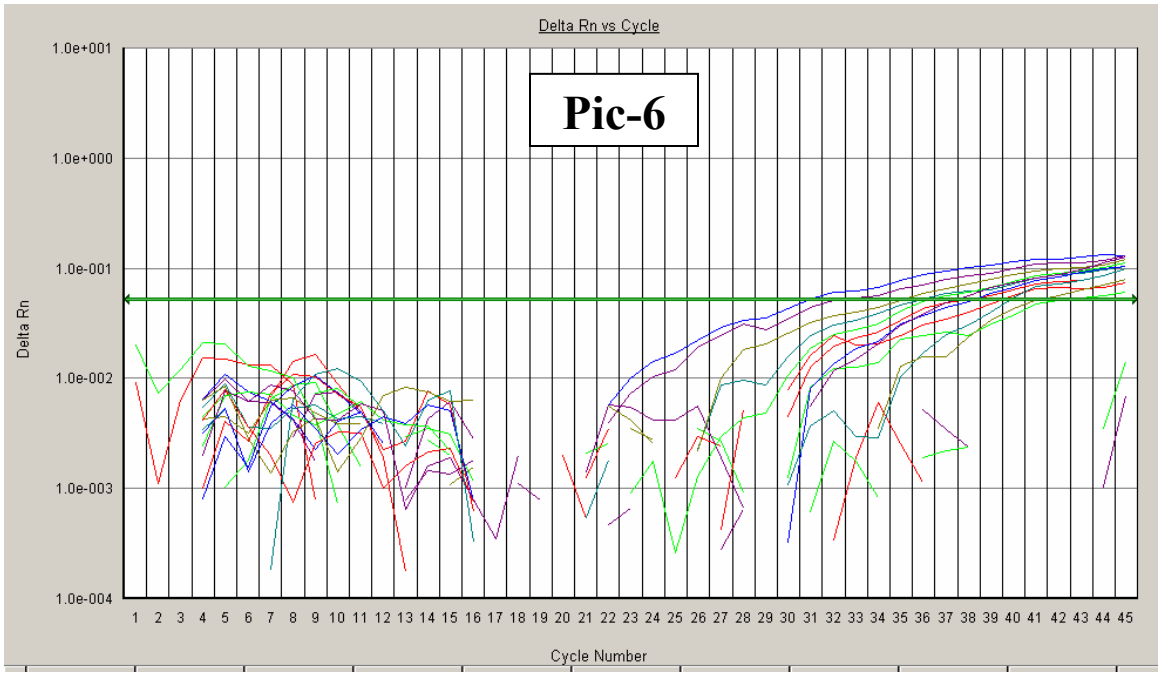

Figure 7. RT-PCR amplification plots for RV-66 RNA using (A) Pic-5 and (B) Pic-6 MGB probes.

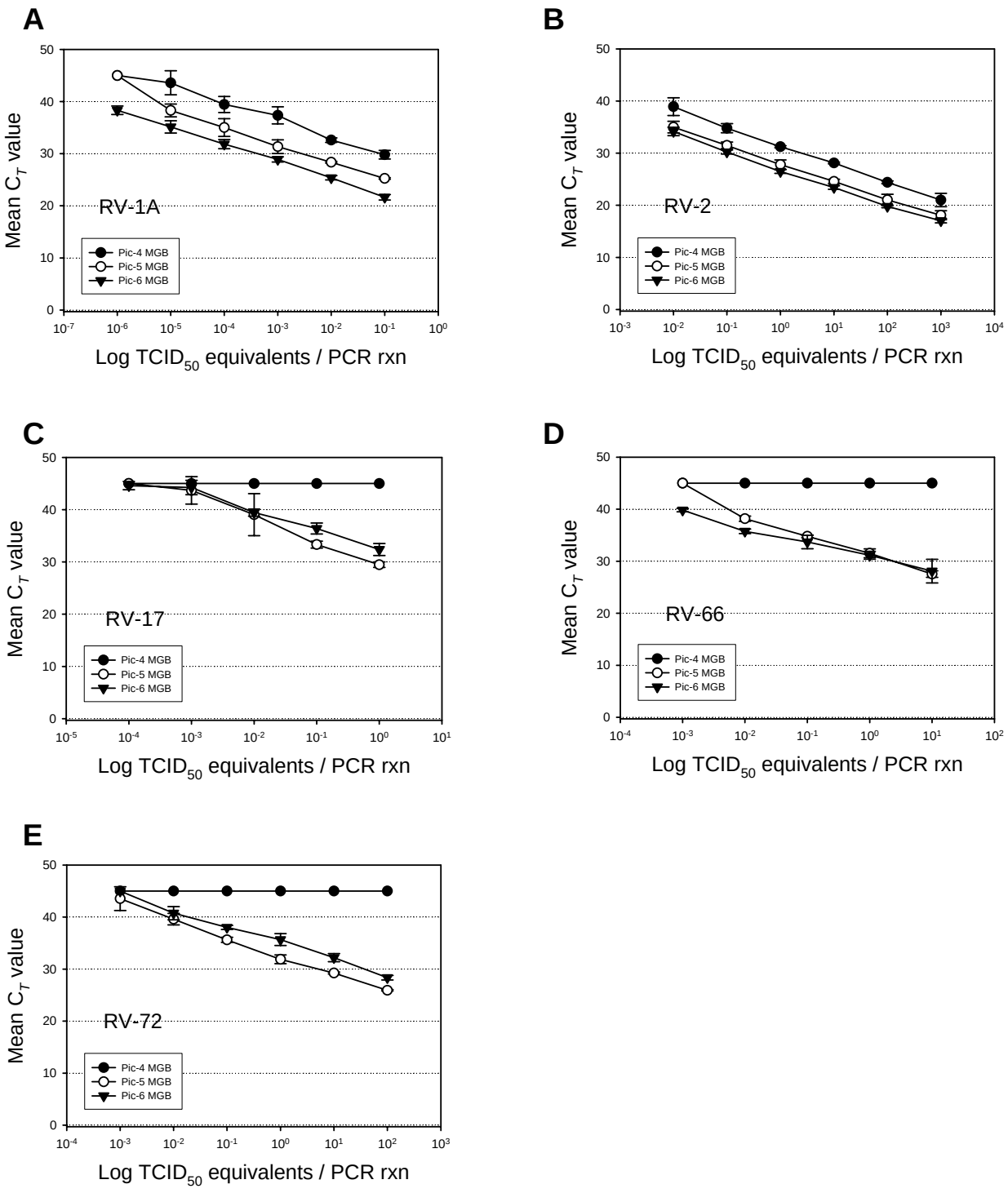

Figure 8. C_T measurements by 3 probes for RV-1A, RV-2, and RVs not detected by Pic-4.

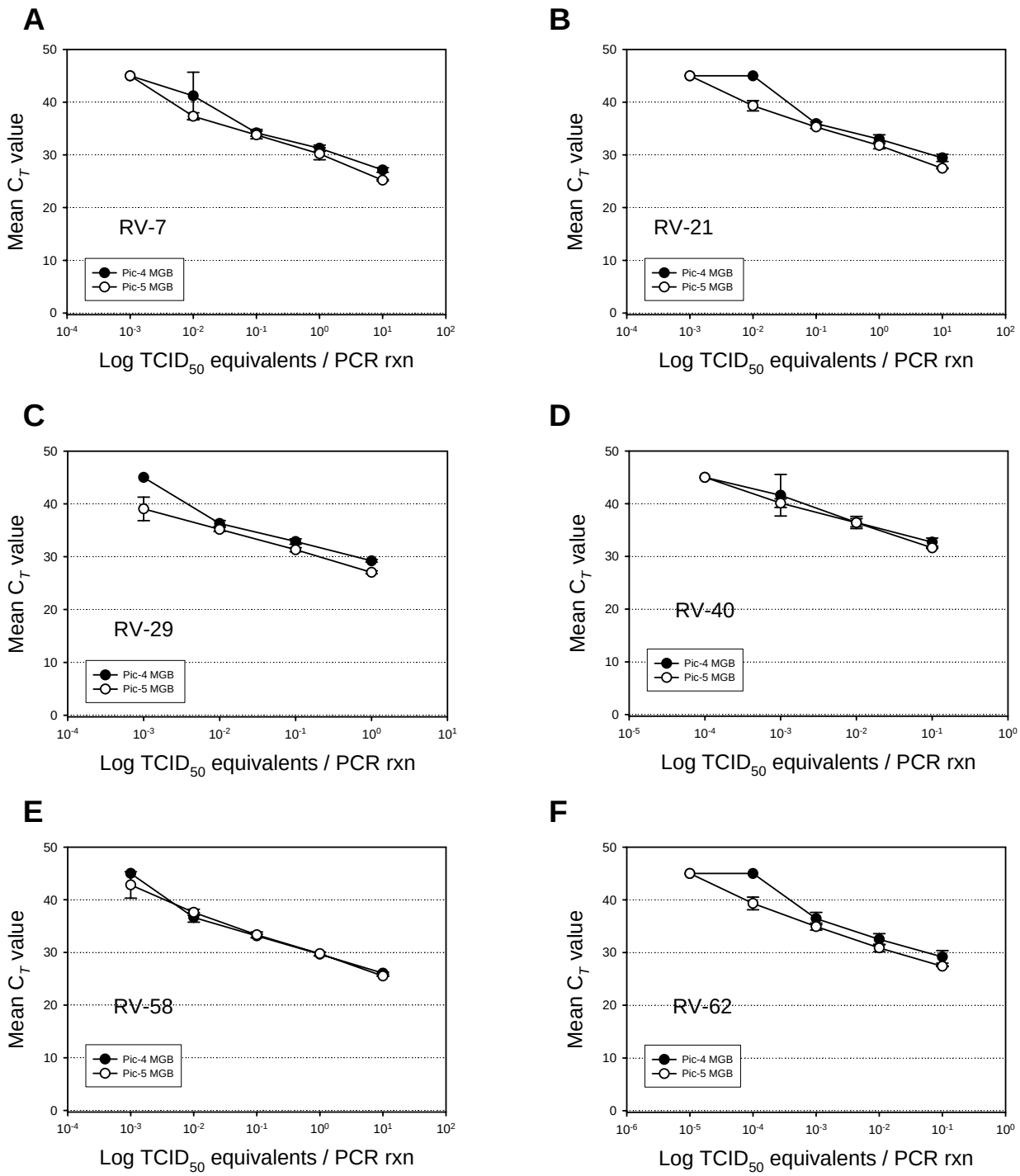

Figure 9. C_T measurements for RVs with either no mismatches or suspected of having no mismatches with the Pic-4 MGB probe. Strain RV-40, which does not have target sequence information, is grouped here because of the similarity of its ΔR_n pattern to the patterns found with the strains known to have no mismatches. RV-2, which also contains no mismatches, is not included here because it was used for the 3 probe comparison study in Figure 8.

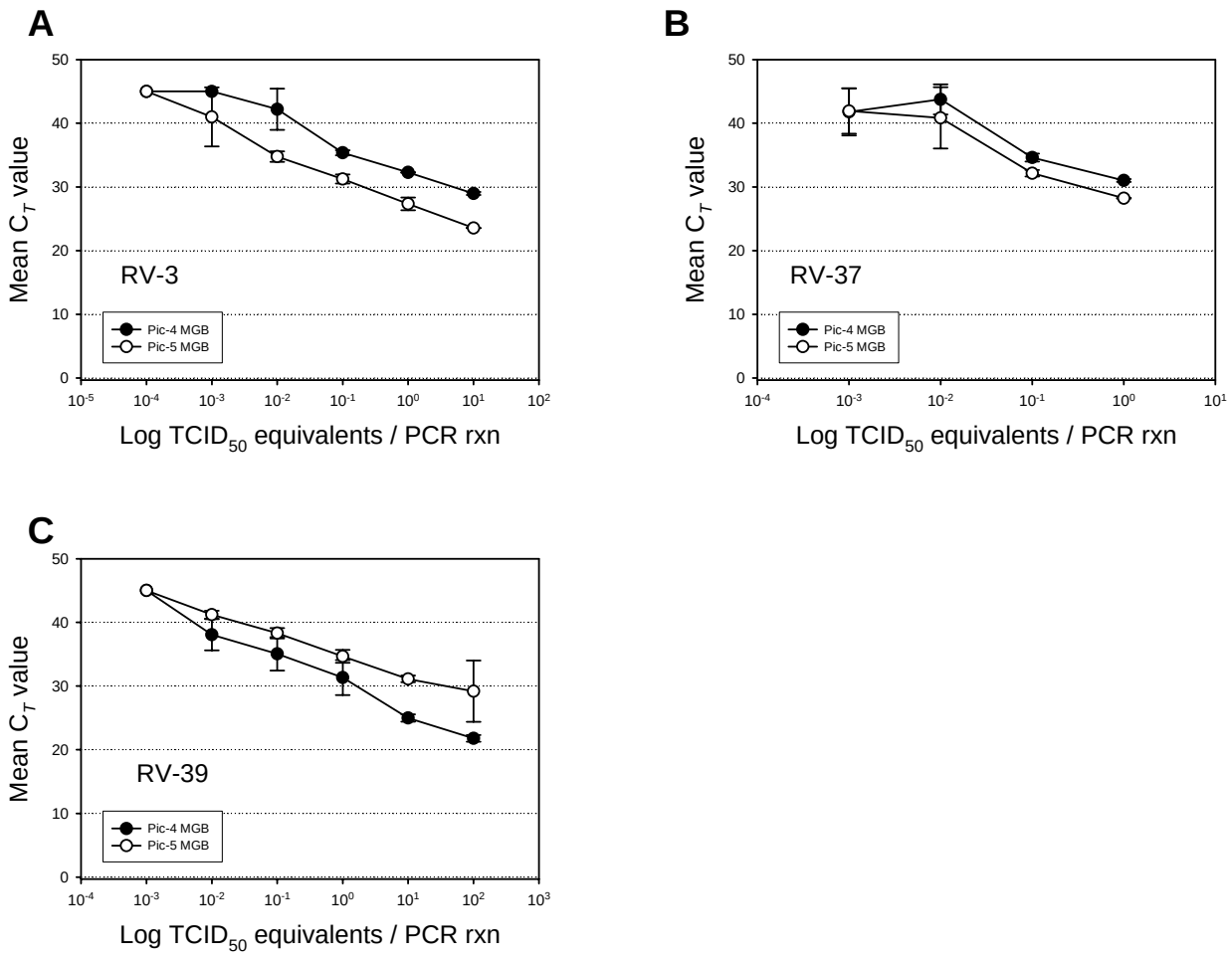

Figure 10. C_T measurements for RVs with either at least 1 mismatch or suspected of having at least 1 mismatch with the Pic-4 MGB probe. Strain RV-3, which does not have sequence information, is grouped here because of the similarity of its ΔR_n pattern to the patterns found with the strains known to have 1 mismatch. RV-66, also suspected of having at least 1 mismatch with the Pic-4 probe, is not included here but in the 3 probe comparison study shown in Figure 8. Strains 1A, 17, and 72 have at least 1 known mismatch but are not shown here for the same reason as RV-66.

3. Sensitivity analysis of the RV RT-PCR assay using a plasmid construct

A 4-kb plasmid containing the RV-2 PCR product was constructed using a commercial cloning kit (Invitrogen; Carlsbad, CA). The initial plan of action was to use the RV-2 amplicon that was produced from a RT-PCR experiment using normal thermocycler parameters as the template DNA. However, the plasmid produced from this approach was not detected by the RT-PCR assay using Pic-4. It was realized afterward that the standard RT-PCR thermocycler parameters did not include a final PCR extension step at 72°C for 7 min, as suggested by the manufacturer's instructions. The lack of PCR extension did not produce the 3′-A overhangs on the amplicon required for proper ligation into the vector which contained 5′-T overhangs. Therefore, the RV-2 amplicon produced by RT-PCR was used as the DNA template for PCR conditions given in the Invitrogen kit, which included the 72°C extension as the final step. The resulting PCR product was then used for the ensuing cloning reactions to successfully produce a plasmid containing the RV-2 amplicon insert (Figure 11).

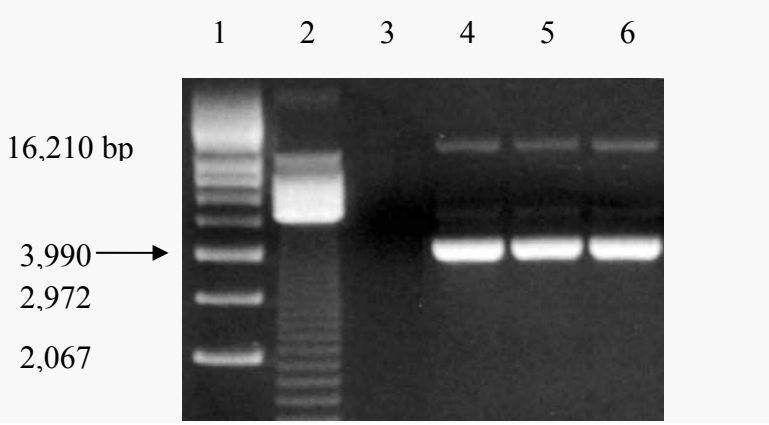

Figure 11. Detection of a plasmid containing the RV-2 target sequence by agarose gel electrophoresis. Lane 1, supercoiled DNA ladder; Lane 2, 123 bp DNA ladder; Lane 3, no vector control; Lanes 4 to 6, plasmid purified from three different *E. coli* transformants.

Analysis by agarose gel electrophoresis revealed the presence of a 4-kb band consistent with the plasmid product containing the 120-base RV-2 insert. Faint bands of higher molecular weight were also observed above the bands representing the plasmid, which suggested the presence of other DNA products. Gel-purification of the plasmid did not exclude these higher molecular weight bands when visualized by agarose gel (data not shown). The origin of these bands is unknown, but they may be the result of the aggregation of circular plasmids linked as concatemers or different forms of the plasmid resulting from supercoiling.

The plasmid was used to compare the analytical sensitivity of the RT-PCR assay using both the Pic-4 and Pic-5 probes. Serial 10-fold dilutions of the plasmid were prepared in DEPC-H_2O containing 30 µg/ml yeast tRNA, and 5 µl from these dilutions were tested in duplicate reactions. The results with both probes are summarized in Table 5, which indicates that the mean lower limit of detection for the plasmid is approximately 30 copies/RT-PCR reaction. Standard curve analyses of the plasmid yielded similar mean efficiency values for both Pic-4 and Pic-5 (86.4% and 92%, respectively) (Table 5). These values are lower than those determined using RV-2 RNA (i.e., mean = 100.2% from six randomly selected assays). The reason for the reduced efficiency measured when using plasmid DNA compared to RV-2 RNA is unclear but could be related to supercoiling of the plasmid. Nevertheless, these results suggest that the RT-PCR assay is very sensitive and is capable of detecting low copies of target. Additionally, there are no differences in the analytical sensitivity or the efficiency of the RT-PCR assays with the two MGB probes.

4. The RT-PCR assay using the Pic-4 and Pic-5 MGB probes is specific for RVs

Since the Pic-1 and Pic-3 primers are not specific for RVs and can amplify the closely related EVs, the analytical specificity of both the Pic-4 and Pic-5 MGB probes was assessed by testing purified RNA from 9 different strains of EV. None of the EVs were detected with either probe, and all EV strains were positive in a real-time RT-PCR assay using an EV-specific probe (Table 6). These results indicate that the RT-PCR assay using either the Pic-4 or Pic-5 MGB probe is specific for RVs, consistent with the finding that none of the Pic-4 and Pic-5 probe sequences scored as perfect matches with EV sequences deposited in the GenBank database.

As the specimens for RV detection in a clinical setting may include nasal aspirates, throat swabs, nasopharyngeal aspirates, bronchoalveolar lavages, etc., which may contain human DNA, DNA purified from a human CEM cell line was tested in the RT-PCR assays with the Pic-4 and Pic-5 MGB probes and yielded no detection (Table 7).

To evaluate the detection of bacteria that could be found in the human nasopharynx, purified DNAs from a panel of 20 gram-positive and gram-negative bacterial species was tested in the RT-PCR assay using the Pic-4 and Pic-5 probes. None of these bacterial DNA samples yielded a positive result, and all samples were confirmed to be of bacterial origin by testing in the 16S rRNA eubacterial PCR assay (Table 7). *Candida albicans*, a fungus commonly found in the nasopharynx of humans, also yielded a negative result in both assays.

Analytical specificity of the RV RT-PCR assay was also assessed by testing non-picornaviral DNA and RNA viruses that may be found in the human nasopharynx, such as adenovirus, influenza virus types A and B, human metapneumovirus, and respiratory syncytial virus. All of these viruses and others tested negative by RT-PCR using both RV-specific probes Pic-4 and Pic-5 (Table 7).

Taken together, the results of these studies show that the RT-PCR assays with Pic-4 and Pic-5 are specific for RVs and will not detect other DNA or RNA sources that may be found in the human nasopharynx. It is also concluded that there are no differences in the assay specificity between the Pic-4 and Pic-5 probes.

5. RT-PCR measurements are comparable on the ABI Prism 7700 and 7000 sequence detection systems

A 10-fold dilution series of RNA from RV-2 was tested on both the ABI 7000 and ABI 7700 Sequence Detection Systems. Table 8 shows the mean C_T values from the duplicate reactions obtained from both instruments. There was little difference observed between the means of the C_T values from the 7000 and 7700 instruments, and both instruments detected RV-2 RNA down to the same endpoint dilution of 10^{-5}. These results suggested that the detection capabilities of the two ABI systems are similar.

A 10-fold dilution series of RV-39 RNA was detected at 10^{-2} $TCID_{50}$ equivalents/PCR reaction on the 7000 instrument and 10^{-3} $TCID_{50}$ equivalents/PCR reaction on the 7700 instrument (Table 9), and the mean C_T values from the 7000 and 7700 instruments were similar. Taken together, the results of these experiments suggest that the detection limits for RV are similar for the two instruments.

B. Real-time RT-PCR detection of human RV in nasal aspirate (NA) specimens

1. Determination of RV detection limits in neat and supernatant NA samples

Detection limits of RV seeded into neat and supernatant NA samples. Purified RNAs from neat and supernatant samples from a NA pool were tested by the RT-PCR assay using the Pic-4 probe. TTable 10T shows that RV-2 was detected in both neat and supernatant samples at the lowest concentration tested, 1 TCID50 genome equivalents/ml. The mean CT values (i.e., 39.8 and 39.4, respectively) obtained from these samples, in theory, correspond to about 1 input copy of RV RNA/PCR reaction. The difference between the means of the CT values from neat and supernatant NA samples was not statistically significant ($p > 0.5$, paired student t-test). The ΔRn values were also comparable and did not differ significantly ($p > 0.3$).

Detection limits for natural RV in neat and supernatant NA samples. Testing of neat and supernatant samples from a second NA pool containing natural RV by the RT-PCR assay using probe Pic-4 demonstrated no appreciable difference in the dilution of RV in the neat and supernatant samples (TTable 11).

These results suggest that RV detection in NA material is highly sensitive and that the lower limit of RV detection in neat and supernatant NAs appears similar. Furthermore, since it is simpler to test neat material than supernatant, and testing of supernatant may not detect RV entrapped in human cells and/or mucous, the testing of neat NA specimens is recommended over supernatant derived from NA specimens.

2. Determination of the RV positivity rate in young school-aged children with upper respiratory tract infection symptoms

Description of study subjects in the Group A Streptococcal Study. A total of 28 subjects participated in this study. The subjects had a mean age of 9.1 years (median, 9.2 years and range, 5.6 to 12.7 years); 67.9% were females; 85.7% were Caucasians; 7.1% were Asians; 3.6% were African Americans; and 3.6% were Hispanics.

A total of 48 NA specimens were obtained from the subjects. A single specimen was obtained from 14 subjects, two specimens were obtained from 10 subjects, three specimens were obtained from three subjects, and five specimens were obtained from one subject. From subjects who had more than one specimen obtained, the mean of the interval between consecutive collections was 23.9 days (median, 21.0 days and range, 4 to 71 days).

Signs and symptoms of URTI were documented within 7 days of collection of the NA specimens in all of the subjects. In 95.8% of the specimen collections, the signs and symptoms had been recorded either the same day or within 3 days before the collection of the NA specimens. These records showed that all of the subjects had slight to mild degrees (i.e. rated as 1 to 2 on a 5-point scale with 0 representing absence and 5 representing the highest degree) of pharyngeal erythema, tonsillar erythema, tonsillar exudate, nasal discharge, sore throat, and cough near the time that the specimens had been collected; only one subject had an elevated temperature (i.e., 99.1°F).

Detection of human RV and *Streptococcus pyogenes* during illness. All 48 NA specimens were tested in the RV RT-PCR assay using the RV-specific MGB probe Pic-5. A total

of 8 (16.7%) of the NA specimens were identified as positive for RV. The positive samples were obtained from different subjects. A throat swab specimen collected from one of these subjects on the same day as the NA specimen yielded light growth of *Streptococcus pyogenes* on culture. A total of 9 (18.8%) of the throat swab specimens collected near the time of the NA specimen yielded growth of *S. pyogenes* by culture. Two subjects each had two throat swab specimens that yielded growth of *S. pyogenes*. Overall, RT-PCR detected RV in 28.6% of the subjects and culture detected *S. pyogenes* in 25.0% of the subjects. These findings suggest that the frequency of RV infection in young school-aged children with symptoms consistent with an upper respiratory tract infection during the fall to early winter months is at least as high as the frequency of *S. pyogenes* infection. Furthermore, dual infection with these two agents appears to be uncommon.

Evaluation of RNA purifications derived from NA specimens for inhibition of RT-PCR. Testing of the purified RNA samples isolated from the 48 clinical NA specimens in RT-PCR reactions containing RV-2 RNA yielded a mean C_T value ± S.D. of 21.1 ± 0.8. Similarly, the DEPC-H_2O control reactions yielded a mean C_T value of 20.8 ± 0.6. These results showed no evidence of inhibition of the RT-PCR assay by the RNA samples derived from the NA specimens.

VI. DISCUSSION

Previous RT-PCR assays described for RV detection have often involved time-consuming techniques such as nested PCR, restriction enzyme digestion, and liquid-phase hybridization, which were run in parallel to further distinguish RVs from the closely related EVs (3, 9, 19, 29, 30, 43). This approach not only demands additional labor that diminishes the usefulness of such assays, but also introduces the opportunity for post-handling contamination of the RT-PCR product. Real-time RT-PCR assays utilizing TaqMan probe chemistry simplifies RV detection and increases sensitivity to a much greater degree (13), but some assays have failed to fully differentiate between RVs and EVs (31, 33, 39), both of which share homology in the 5′ NCR region. Additionally, a high degree of variability within the 5′ NCR region exists among members of the RV genus. Indeed, a major obstacle in the development of molecular diagnostic assays for the detection of RV is the broad diversity of RV serotypes and clinical isolates (14).

The present study is the first to evaluate the potential use of a fluorescent TaqMan MGB oligonucleotide probe in a real-time RT-PCR assay for the detection of RV via the 5′ NCR. The assay has been demonstrated to be less laborious than virus isolation, relatively rapid (approximately 5 h in a single work day, compared to days to weeks for viral culture), sensitive, and specific for RV. One of the main advantages of using TaqMan MGB chemistry over conventional TaqMan probes is the overall length of the final oligonucleotide. Because the MGB ligand effectively increases the probe T_m due to its high affinity to bind DNA, the length of the probe can be much shorter (13 to 20 bases) compared to standard TaqMan probes (typically 18 to 40 bases). The second main advantage of MGB probe chemistry exploits the novel 3′ non-fluorescent quencher (or dark quencher), which gives a significantly lower fluorescent background (2).

The sensitivity of RV detection using MGB probes depends largely on the presence of DNA base mismatches between the probe sequence and target sequence (Figures 4 to 6). This conclusion is supported by the known fact that MGB probes are sensitive to single base mismatches (32) and have been used to detect point mutations (56) and single nucleotide polymorphisms (53), as well as for allelic discrimination (51). The initial MGB probe Pic-4 strongly detected the RV strains with perfect target base matches to the probe sequence (i.e., strains 2, 7, 21, 29, 58, and 62) with ΔR_n values approaching 3.0, which are typical for the prototype strain used in this study, RV-2 (Figures 4B and 5). Conversely, RV strains containing one or more base mismatches with the Pic-4 sequence had dramatically reduced ΔR_n reporter signal or no signal at all (Figures 4A, C-E and 6).

It is interesting that the assay with Pic-4 detected RV-1A (albeit weakly) but did not detect RV-17 and RV-72 (Table 4). These three strains each have two mismatches, one being at position no. 1 (Table 3). Therefore, mismatches at a position in addition to position 1 may be important for detection of the RV targets. The next base mismatch from the 5′ end of the probe for RV-17 is at position 11 and for RV-72 is at position 10. These mismatches are located toward the middle of the probe annealing site. In contrast, the next base mismatch from the 5′ end of the probe for RV-1A is located farther downstream at position 14, only 3 bases from the MGB ligand (Table 3). Perhaps, the strong affinity of the MGB ligand for DNA compensated for the mismatch at position 14 in RV-1A, whereas the mismatches in RV-17 and RV-72 may be located too far from the MGB ligand for it to compensate for these mismatches.

As for the RV-87 target, it appears to have too many mismatches for it to hybridize with Pic-4 (Table 3). However, one of the assumptions made in these studies is that the primer set, Pic-1 and Pic-3, is effective for amplification of the RV targets. Analysis of the RV-87 5′ NCR

sequences deposited in Genbank reveals that the sequences of the primer annealing sites have no base mismatches with the primers, implying that the primers are indeed effective for amplifying the target sequence for this strain. It is recommended, nevertheless, to analyze the PCR products from RV-87 and other RVs by agarose gel electrophoresis to confirm the assumption that the primers are successfully amplifying the target sequence.

Probe Pic-5 was designed to improve the detection of RV strains having mismatches with Pic-4. The three degenerate bases in Pic-5 at positions 1, 10, and 11 were considered to be the most critical positions and would cover the most common polymorphisms in the RV strains that have been presently sequenced. Analysis of the 5′ NCR sequences of 65 RV serotypes and clinical isolates identified in Genbank indicated that 40 (61.5%) of the strains have perfect matches with Pic-5. It was hypothesized that *Pic-5, which accommodates the positions of the most frequent base polymorphisms in RVs, would offer the best chance for detecting most if not all RV strains*. The results from this study support this hypothesis, with 14/15 (93.3%) RV strains being successfully detected by the assay with Pic-5 (Table 4).

In general, the assay with Pic-5 detected RVs containing base mismatches to the Pic-4 probe sequence better than the assay with Pic-4, although the ability to detect more RVs came with an overall sacrifice in ΔR_n reporter signal (Figures 4 to 6). Low ΔR_n values measured by the assay with Pic-5 were especially apparent with RVs containing perfect target sequence alignments to Pic-4 (i.e., strains 7, 21, 29, 40, 58, and 62) (Figure 5). This phenomenon may be explained by the nature of degenerate probes. There are 8 different probe combinations possible with the three degeneracies contained within Pic-5, and only one of the probes in the combination will anneal perfectly to a particular RV target sequence. Some of the remaining probes in the combination may not anneal or may anneal only partially. In these situations either

no reporter signal is generated or a reduced signal may be generated from the probes with mismatches. *The reduction in the proportion of probes in the combination that can anneal perfectly may therefore lead to a reduction in overall reporter signal*. In contrast, the detection of RV strains with perfect target sequence alignment with a non-degenerate probe (i.e., Pic-4) will yield higher ΔR_n reporter signal values than for a degenerate probe combination (i.e., Pic-5) (i.e., strains 7, 21, 29, 40, 58, and 62) (Figure 5).

Probe Pic-6 was designed in an attempt to address the low ΔR_n reporter signal values observed with Pic-5. The rationale for the single degeneracy at the first 5′ position of the probe sequence was based on the ability of Pic-5 to detect three of the strains previously undetected by Pic-4 (17, 66, and 72), as well as the atypically low ΔR_n reporter signal by Pic-4 for strain 1A. As mentioned previously, strains 1A, 17 and 72 all have a T to C mismatch at position 1; sequence information is unavailable for RV-66, but this strain likely has a T to C mismatch at the first position as well. Because these strains were all detected by Pic-5, it was hypothesized that *the first 5′ nucleotide position was the most critical for probe annealing, and that a probe degeneracy at this position would be sufficient to allow detection of all 15 RV strains while retaining the higher ΔR_n reporter signal achieved by Pic-4*. Therefore, RV strains that were not detected or weakly detected by Pic-4 were tested by Pic-6. Only strain 1A supported this hypothesis, while the other strains showed that Pic-5 generated higher ΔR_n reporter signal than Pic-6 (Figure 4). The data suggests that *although the first 5′ position is vital to generation of a reporter signal for detection of RV, the positions of other mismatches are a determinant for the magnitude of the signal.*

Taken together, these observations make sense in light of the sensitivity of MGB probes to single-base mismatches and lead to the following conclusion: *the more perfectly aligned the*

target and probe sequences, the better the duplex is stabilized for PCR processing and subsequent fluorescent reporter generation. The level of ΔR_n reporter signal also seems to depend on the number of degeneracies within the probe, as evidenced by the higher ΔR_n reporter signal with Pic-6 in strain 1A compared to Pic-5, even though neither probe covers the next downstream base mismatch at position 14 (Table 3). C_T measurements for RV-1A confirm that Pic-6 is the better probe (Figure 8A). Again, this occurrence may be explained by the nature of degenerate probes: although both Pic-5 and Pic-6 account for the first position T to C mismatch in RV-1A, there is a greater quantity of the Pic-6 probe available to bind to the target than with Pic-5 since these degenerate probes consist of two and eight combinations, respectively. The same explanation can be applied to RV-39, in which the non-degenerate Pic-4 probe detected this strain with both a higher ΔR_n value (Figure 6C) and lower C_T value (Figure 10C) than with Pic-5. The only exception to this inference, ironically, seems to be with the prototype strain for this study, RV-2 (Figure 4B). Pic-4 and Pic-6 differ only by the first nucleotide (Table 3). The reason why Pic-6 produces a higher ΔR_n reporter signal than Pic-4 for RV-2 remains unclear.

In conclusion, the Pic-5 probe was the most promising MGB probe for detection of the selected set of RVs, and further studies were performed using this probe in the RT-PCR assay.

The lower limits of detection for 14 RV strains were determined to be ≤ 0.01 $TCID_{50}$ genome equivalent units/RT-PCR reaction (Table 4). An analytical comparison of the sensitivity of RV detection between RT-PCR and viral cell culture indicates that the RT-PCR assay is more sensitive for detecting the presence of the RV genome in 12/14 (85.7%) RVs detected by probe Pic-5 (Appendix B). This difference in sensitivity between the RT-PCR and culture methods may be caused by the presence of noninfectious or otherwise defective virus particles that were present in the viral cell culture suspensions.

The assay clearly demonstrated specificity for RV when a selection of purified nucleic acids from human cells, EVs, and bacterial and other viral agents found in the human nasopharynx all tested negative (Tables 6 and 7). The most important conclusion from this set of studies is that *there is no cross-reactivity of detection between RVs and EVs in the RT-PCR assay*, one of the major difficulties in the development of RV-specific molecular assays. Since the primer set is capable of amplifying RNA from EVs as well as RVs, the specificity of the assay is due solely to the sequence specificity of the MGB probe. A BLAST query within the GenBank database revealed no hits with EVs for any of the three probes. Based on genetic analyses of both the 5′ NCR and the VP1 gene reviewed in the literature (14), it appears that the 5′ NCR of the RV genome is a more conserved target for RV detection. However, given the high mutation rates of RNA viruses, continued surveillance of RV strains circulating in the community is still required to make certain that molecular-based detection assays are updated.

The RT-PCR assay was able to clearly identify 8/48 NA specimens that were positive for RV, which correlates to about 29% of the pediatric subjects. This percentage is slightly higher than the estimated 10-25% of cases of RV-mediated common colds in children (6). The cases were detected between the months of October and February, in accordance with the peak period of the year in which RV is most active.

A technical aspect borne out of these results is that nasal aspirates are suitable clinical specimens from which to isolate RV RNA. However, one limitation of this study was that the detection limits of RV-2 determined in NA specimens were performed with the Pic-4 probe rather than the Pic-5 probe. This set of experiments had been done earlier in the study, before the disadvantages of Pic-4 were realized. Still, Pic-5 was able to positively identify several NA

samples that were previously detected in those experiments, confirming that Pic-5 had at least the ability to detect RV in the same NA samples that Pic-4 had detected.

The evaluation of RT-PCR inhibition by purified RNAs derived from the NA specimens showed no indication of the presence of inhibitors. However, the concentration of seeded RV-2 RNA in the master mix that yielded a C_T value of approximately 21 corresponds to 10,000 $TCID_{50}$ genome equivalents/RT-PCR reaction of RV-2 RNA. Such a high input of target RNA may have made the evaluation of small amounts of inhibition of the RT-PCR difficult. A future study to address this aspect is recommended to explore the use of a smaller input of RV RNA in the master mix in order to detect lower amounts of inhibition.

Lastly, an alternative explanation for the differences in detection of the RV strains used in this study is that base mismatches between the RV target sequences and the primer sequences themselves could exist. In addition to the mismatches with the probe sequences, inefficient priming of the RV target sequences may also participate in the reduction of assay sensitivity to RV strains. This is an issue that was not fully addressed. A BLAST search analysis of the Pic-1 and Pic-3 primer sequences had revealed a small number of RV strains that contained base mismatches with the Pic-1 forward primer. However, sequencing information for the Pic-3 reverse primer annealing site is lacking for many RV 5′ NCR sequences deposited in the GenBank database. More sequencing data is needed before this concern can be resolved.

Ideally, a real-time RT-PCR assay for the detection of RV would utilize a single oligonucleotide probe capable of detecting all RVs. So far only one group has approached this ideal through the use of two TaqMan probes (14). The probes used in that study also targeted the 5′ NCR, but at nucleotide positions 302 to 321 relative to the sequence of RV-2, farther upstream to the positions that Pic-5 targets in this study (positions 452 to 467). These two probes were able

to detect all 29 RV serotypes and 48/58 (82.8%) RV clinical isolates evaluated. However, the assay employed in that study was a two-step RT-PCR, which is more cumbersome than the one-step RT-PCR assay developed in this study. In addition, the cost of two TaqMan probes is approximately double the cost of a degenerate MGB probe. Further studies should be done to compare that assay with the assay using Pic-5 to detect the RV strains evaluated in this study.

Based on an analysis of the available RV 5′ NCR sequences (n = 147) deposited in GenBank as well as the RV strains detected in this study, it was found that the Pic-5 MGB probe has the capability to detect 23 serotypes and 22 clinical isolates (45/147 = 30.6%) of RV (Appendix C). *The potential to detect additional RVs containing mismatches not covered by the Pic-5 probe has been demonstrated by the detection of RV-39 in this study*. Further studies evaluating additional RV serotypes are needed to validate this hypothesis. The Pic-5 degenerate probe, with 8 different probe combinations, is far from the ideal detection system, but alternatively Pic-5 possesses greater versatility when dealing with the variability seen among RVs. There is, however, an increased chance of non-specific detection in employing a RT-PCR system using 8 different probes, which could be a disadvantage to favoring the use of such degenerate probes.

Nonetheless, the high degree of specificity and analytical sensitivity of the Pic-5 probe, coupled with the rapid and less laborious setup and run times, makes the RT-PCR assay developed in this study a more practical diagnostic tool than viral culture for the detection of RV in a clinical setting. Sample preparation for the assay with 72 reactions takes on average about 3 h followed by a 2.5 h RT-PCR, which translates into available results in about a full work day's time, compared to days or weeks for viral culture. The assay also has advantages over current real-time RT-PCR assays for the detection of RV in the use of an MGB probe, which is highly

sensitive to single base mismatches. This sensitivity is demonstrated in the MGB probe comparison studies which show that one base mismatch is enough to cause a measurable reduction in reporter signal (compare ΔR_n reporter signals for RV-37 and RV-2 by the Pic-4 probe, Figures 6B and 4B, respectively). For the development of forthcoming RT-PCR assays that will continue to detect an increasing number of RV serotypes with polymorphic nucleotide sequences, the discrimination of single base mismatches will be critical.

VII. FUTURE PERSPECTIVES AND PUBLIC HEALTH SIGNIFICANCE

Although the work presented in this thesis has addressed many key points that take precedence in the development of a real-time RT-PCR for the detection of RV, there is still much work to be done before the assay can be considered for use in a genuine clinical setting.

A large degree of the advancement effort depends on additional RV sequencing information. As of July 2005, the complete genomes of only five human RV serotypes (i.e., 1B, 2, 14, 39, and 89) and the full 5′ NCR sequences of only nine additional serotypes (i.e., 1A, 7, 21, 29, 37, 58, 62, 72, and 87) have been sequenced and deposited in GenBank. Despite the versatility of the Pic-5 MGB probe to detect the representative RV strains used in this study, it is impossible to tell if Pic-5 can detect a high proportion of all RV strains that circulate in the community without having the sequence information for the other 87 or more serotypes as well as recent isolates from geographically diverse areas. Antigenic variants of RV serotypes are constantly emerging (42), and updating molecular assays such as RT-PCR for RV detection will depend on the continuous genetic surveillance of these variants. Therefore, it is vital to obtain sequence information on the existing RV serotypes as well as ongoing clinical isolates.

Further work more pertinent to this study would be to assess the efficiency of the Pic-5 probe in detecting additional strains of RV. Serotypes 1B, 14, and 89 should be included in a forthcoming panel of RVs for testing since the 5′ NCR sequences of these serotypes are already known. A collection of nine RV serotypes (i.e., 18, 36, 39, 41, 42, 43, 47, 52, and 58) provided by the Children's Hospital of Columbus, as well as a number of clinical isolates of RV, should also be included in the panel. The rationale for inclusion of the latter is that many of the RV serotypes catalogued by the ATCC were isolated from human specimens during the 1960s.

Given that RVs can mutate rapidly, it is important to evaluate the RT-PCR assay in the detection of RVs that currently circulate throughout a human population.

Any additional assessment of the incidence RV infection within a study group is recommended to have a larger sample size, which would increase the robustness of any epidemiological findings that might be revealed.

Some technical aspects of the RT-PCR assay also warrant further investigation. The possibility of the primer set used in this study having mismatches with RV strains needs to be investigated. Moreover, an evaluation of NA specimens for RT-PCR inhibition needs to be undertaken using a lower input of RV-2 RNA (1 $TCID_{50}$ genome equivalents/RT-PCR reaction) to evaluate purified RNA samples derived from the NA specimens for the presence of relatively low levels of RT-PCR inhibitors. Lastly, a comparison of the RT-PCR assay developed by Deffernez et al. (14) and the RT-PCR assay developed in this study may be of interest, particularly in the capabilities of the respective probes to detect RVs.

The results and conclusions drawn from this study have several implications from a public health standpoint. One of the potential applications of the RT-PCR assay was to use it as a diagnostic tool to rule out RV infection in patients displaying cold-like symptoms and who are positive for *S. pyogenes* infection, thereby investigating the role of *S. pyogenes* as a causative agent of the common cold. However, based on the results from this study, it is apparent that the RT-PCR assay for RV detection has yet to be finalized as a diagnostic tool. Until an assay is shown to detect all RVs, one cannot rule out RV infection in patients displaying cold-like symptoms. A more global contribution provided by this study is the potential for a more rapid and reliable diagnosis of RV infection in the clinical setting, which can affect the avenue of therapy. RVs are no longer simply the causative agents of the common cold. With the occurrence

of more serious illnesses associated with RV in immunosuppressed populations on the rise, it is imperative that infection with RV is quickly diagnosed early in the disease progression in order to apply clinically effective antiviral treatments, such as the potential use of Pleconaril (4, 15), to reduce the duration and severity of disease for severely immunocompromised patients.

APPENDIX A: Tables

Table 1. Description of picornavirus strains and stock suspensions used in this study

Picornaviridae	Serotype	ATCC no.	Virus titer of stock suspension ($TCID_{50}$ / 0.1 ml)[a]
Rhinovirus			
Major Group	3	VR-1113	$10^{-4.0 \pm 0.6}$
	7	VR-1117	$10^{-4.5 \pm 0.3}$
	17	VR-1127	$10^{-3.6 \pm 0.1}$
	21	VR-1131	$10^{-3.9 \pm 0.6}$
	37	VR-1147	$10^{-4.4 \pm 0.1}$
	39	VR-340	$10^{-4.9 \pm 0.5}$
	40	VR-1150	$10^{-3.9 \pm 0.5}$
	58	VR-1168	$10^{-4.2 \pm 0.1}$
	66	VR-1176	$10^{-3.5 \pm 0.4}$
	72	VR-1182	$10^{-4.4 \pm 0.0}$
Minor Group	1A	VR-1559	$10^{-2.3 \pm 0.3}$
	2	VR-1112	$10^{-4.5 \pm 0.0}$
	29	VR-1139	$10^{-4.1 \pm 0.5}$
	62	VR-1172	$10^{-2.5 \pm 0.0}$
Rhinovirus 87	87	VR-1197	$10^{-4.4 \pm 0.2}$
Enterovirus			
Coxsackievirus	B-1	VR-1032	N.D.
	B-3	VR-30	N.D.
Echovirus	3	VR-1040	N.D.
	4	VR-1041	N.D.
	6	VR-1044	N.D.
	7	VR-1047	N.D.
	9	VR-1050	N.D.
	11	VR-1052	N.D.
Enterovirus	68	VR-1076	N.D.

[a] $TCID_{50}$, 50% tissue culture infectious dose. Titers are the mean ± S.D. from two separate trials.
[b] N.D., not done.

Table 2. Nucleotide sequences of primers and probes used in this study

Micro-organism and oligo-nucleotide designation	Function	Position and orientation	Sequence (5′ → 3′)[d]
Rhinovirus			
Pic-1	Primer	434→450[a]	TCCTCCGGCCCCTGAAT
Pic-3	Primer	531←553	GAAACACGGACACCCAAAGTAGT
Pic-4	MGB Probe	452→467	TGGCTAACCTTAACCC
Pic-5	MGB Probe	452→467	YGGCTAACCYWAACCC
Pic-6	MGB Probe	452→467	YGGCTAACCTTAACCC
Enterovirus			
Ent 1	Primer	579←597[b]	GATTGTCACCATAAGCAGC
Ent 2	Primer	451→469	CCCCTGAATGCGGCTAATC
Ent 3	Probe	532→557	CGGAACCGACTACTT TGGGTGTCCGT
Eubacteria			
Cor 1	Primer	1320→1341[c]	CCATGAAGTCGGAATCGCTAG
Cor 2	Primer	1413←1431	ACTCCCATGGTGTGACGG
Cor 3	Probe	1395←1369	CGGTGAATACGTTCCCGGGCCTTGTAC

[a] Numbering corresponds to a published sequence of the 5′ NCR for a strain of RV-2 (49).
[b] Numbering corresponds to a published sequence of the 5′ NCR for a strain of EV (37).
[c] Numbering corresponds to a published sequence of the 16S rRNA gene of *E. coli* (17).
[d] IUB Group codes used: Y = C or T; W = A or T.

Table 3. Sequences of the 15 RV strains and 3 MGB probes used in this study relative to a common probe hybridization target among human RVs

Source		Nucleotide at following position numbers relative to the 5′ end of the hybridization target[a]															
		1	2	3	4	5	6	7	8	9	10	11	12	13	14	15	16
RV target sequence		T	G	G	C	T	A	A	C	C	T	T	A	A	C	C	C
RV serotype	GenBank accession. no.																
1A	AF108179	C	.	.	.	.	.	.	.	.	.	.	.	.	A	.	.
2	X02316	.	.	.	.	.	.	.	.	.	.	.	.	.	.	.	.
3	N.A.[b]	–	–	–	–	–	–	–	–	–	–	–	–	–	–	–	–
7	AF108185	.	.	.	.	.	.	.	.	.	.	.	.	.	.	.	.
17	AF542419	C	.	.	.	.	.	.	.	.	.	A	.	.	.	.	.
21	AF108180	.	.	.	.	.	.	.	.	.	.	.	.	.	.	.	.
29	AF108181	.	.	.	.	.	.	.	.	.	.	.	.	.	.	.	.
37	AF108182	C	.	.	.	.	.	.	.	.	.	.	.	.	.	.	.
39	AY751783	.	.	.	.	.	.	.	.	.	.	.	.	.	A	.	.
40	N.A.	–	–	–	–	–	–	–	–	–	–	–	–	–	–	–	–
58	AF108183	.	.	.	.	.	.	.	.	.	.	.	.	.	.	.	.
62	AF108184	.	.	.	.	.	.	.	.	.	.	.	.	.	.	.	.
66	N.A.	–	–	–	–	–	–	–	–	–	–	–	–	–	–	–	–
72	AF108186	C	.	.	.	.	.	.	.	.	C	.	.	.	.	.	.
87	AF108187	C	.	.	.	.	.	.	T	.	C	.	.	.	.	.	A
MGB probe[c]																	
Pic-4		.	.	.	.	.	.	.	.	.	.	.	.	.	.	.	.
Pic-5		Y	.	.	.	.	.	.	.	.	Y	W	.	.	.	.	.
Pic-6		Y	.	.	.	.	.	.	.	.	.	.	.	.	.	.	.

[a] Base identity indicated by a (.) and unknown base indicated by a (−).
[b] N.A., not available.
[c] IUB Group codes used: Y = C or T; W = A or T.

Table 4. Comparison of the detection limits of 15 serotypes of RV measured by three different RT-PCR assays each with a different MGB probe

Rhinovirus serotype	Lower limit of detection[a] ($TCID_{50}$ genome equivalents/PCR reaction ± S.D.) for RT-PCR assay with the following probes:		
	Pic-4	Pic-5	Pic-6
1A	0.000055 ± 0.000064	0.00001 ± 0.0	0.0000055 ± 6.4E-06
2	0.01 ± 0.0	0.001 ± 0.0	0.001 ± 0.0
3	0.055 ± 0.064	0.0055 ± 0.0064	N.D.[b]
7	0.0055 ± 0.064	0.001 ± 0.0	N.D.
17	> 430, > 430	0.055 ± 0.064	0.01 ± 0.0
21	0.1 ± 0.0	0.01 ± 0.00	N.D.
29	0.01 ± 0.0	0.0001 ± 0.0	N.D.
37	0.0505 ± 0.07	0.055 ± 0.064	N.D.
39	0.01 ± 0.0	0.01 ± 0.0	N.D.
40	0.0055 ± 0.0064	0.001 ± 0.0	N.D.
58	0.01 ± 0.0	0.0055 ± 0.0064	N.D.
62	0.001 ± 0.0	0.0001 ± 0.0	N.D.
66	> 370, > 370	0.001 ± 0.0	0.001 ± 0.0
72	> 3000, > 3000	0.01 ± 0.0	0.01 ± 0.0
87	> 3000, > 3000	> 3000, > 3000	> 3000, >3000

[a] Based on two independent experiments. Values for strains yielding negative results presented as greater than the highest input concentration tested. Boxes highlight the assay results for serotypes that changed from negative with Pic-4 to positive with Pic-5 and Pic-6 for RV.

[b] N.D., not done.

Table 5. Detection limits for the RV plasmid and corresponding assay efficiencies

TaqMan MGB probe	Detection limit by RT-PCR[a]	Assay efficiency (%)
Pic-4	33 ± 45	86.4 ± 3.3[b]
Pic-5	30 ± 47	92.0 ± 0.8[c]

[a] Values given are the mean copy number per reaction ± S.D. from four separate experiments.
[b] Based on two separate experiments.
[c] Based on four separate experiments.

Table 6. Results from testing 9 EV strains by RT-PCR assays for RV and EV

Virus tested	Result from following RT-PCR assay[a]:	
	Rhinovirus[b]	Enterovirus
Coxsackievirus B1	–	+
Coxsackievirus B3	–	+
Echovirus 3	–	+
Echovirus 4	–	+
Echovirus 6	–	+
Echovirus 7	–	+
Echovirus 9	–	+
Echovirus 11	–	+
Enterovirus 68	–	+

[a] +, positive result; –, negative result.
[b] RT-PCR was performed with both Pic-4 and Pic-5 MGB probes

Table 7. Results from testing heterologous DNAs and RNAs by real-time assays

DNA or RNA source	Result from following assay:		
	Rhinovirus RT-PCR with:		Eubacterial 16S rRNA PCR
	Pic-4	Pic-5	
Bacterium			
Acinetobacter anitratus	−	−	+
Bordetella pertussis	−	−	+
Corynebacterium spp.	−	−	+
Enterobacter cloacae	−	−	+
Escherichia coli	−	−	+
Haemophilus influenzae	−	−	+
H. parainfluenzae	−	−	+
Klebsiella pneumoniae	−	−	+
Moraxella catarrhalis	−	−	+
Neisseria meningitidis	−	−	+
Neisseria mucosa	−	−	+
Proteus vulgaris	−	−	+
Pseudomonas aeruginosa	−	−	+
Staphyloccus aureus	−	−	+
Staphylococcus spp., coag. neg.	−	−	+
Streptococcus pneumoniae	−	−	+
Streptococcus pyogenes	−	−	+
Streptococcus spp.,			
β-hemolytic (Group B)	−	−	+
β-hemolytic (Group C)	−	−	+
Viridans group	−	−	+
Fungus			
Candida albicans	−	−	−
Virus			
Adenovirus	−	−	N.A.
Human cytomegalovirus	−	−	N.A.
Herpes simplex virus types 1 and 2	−	−	N.A.
Human metapneumovirus	−	−	N.A.
Influenza virus A/B	−	−	N.A.
Parainfluenza virus types 1, 2, and 3	−	−	N.A.
Respiratory syncytial virus	−	−	N.A.
Varicella-zoster virus	−	−	N.A.
Homo sapiens			
CCRF-CEM T-cell line	−	−	N.A.

[a] +, positive; −, negative. N.A., not applicable.

Table 8. Comparison of RT-PCR C_T values measured on the ABI Prism 7000 and 7700 Sequence Detection Systems for RV serotype 2

RV-2 RNA dilution ($TCID_{50}$ unknown)	C_T value[a]	
	ABI 7000	ABI 7700
10^{-2}	29.96 (0.2)	27.83 (0.1)
10^{-3}	33.77 (0.6)	31.11 (0.7)
10^{-4}	38.58 (0.2)	36.10 (0.9)
10^{-5}	40.94 (0.4)	40.34 (6.6)
10^{-6}	Undetected	Undetected

[a] Mean value (± S.D.) from duplicate samples.

Table 9. Comparison of RT-PCR C_T values measured on the ABI Prism 7000 and 7700 Sequence Detection Systems for RV serotype 39

Concentration of RV-39 ($TCID_{50}$ equivalents/PCR reaction)	C_T value[a]	
	ABI 7000	ABI 7700
10^{0}	32.58 (0.1)	30.43 (0.1)
10^{-1}	36.52 (0.4)	34.33 (0.1)
10^{-2}	40.03 (0.5)	41.50 (3.7)
10^{-3}	Undetected	41.59 (0.7)
10^{-4}	Undetected	Undetected

[a] Mean value (± S.D.) from duplicate samples.
[b] N.D., not done.

Table 10. Comparison of RT-PCR assay measurements from testing materials derived from a pool of NA specimens seeded with varying concentrations of RV serotype 2

RV-2 conc. in NA pool ($TCID_{50}$ equivalents/ml)	C_T value		ΔR_n value	
	Neat NA	Supernatant NA	Neat NA	Supernatant NA
10^3	28.1 (0.1)[a]	27.7 (0.2)	2.5 (0.5)	2.3 (0.01)
10^2	30.0 (2.7)	32.2 (0.2)	3.1 (1.8)	2.0 (0.1)
10^1	35.7 (0.2)	35.8 (0.3)	1.2 (0.04)	1.4 (0.2)
10^0	39.8 (1.0)	39.4 (0.2)	0.6 (0.2)	0.8 (0.02)
None	45.0	N.D.	-0.09 (0.0)	N.D.

[a] Mean value (± S.D.) from duplicate samples. N.D., not done.

Table 11. Comparison of RT-PCR assay measurements from materials derived from a pool of NA specimens containing natural RV

NA sample	Trial 1		Trial 2	
	C_T value	ΔR_n value	C_T value	ΔR_n value
Neat	37.1 (0.7)[a]	1.2 (0.1)	37.4 (0.4)	1.6 (0.2)
Supernatant	43.7 (1.6)	0.3 (0.1)	37.1 (0.2)	1.7 (0.1)

[a] Mean value (± S.D.) from duplicate samples.

APPENDIX B

Analytical comparison of the sensitivity of RV detection by RT-PCR and cell culture

Appendix B

Serotype	Detection limit by RT-PCR	Concentration of RV in starting material for positive PCR at endpoint	Calculated no. of $TCID_{50}$ that would be inoculated into a cell culture	Culture result expected[a]
1A	0.00001	0.0008571	0.0001714	–
2	0.001	0.0857143	0.0171429	–
3	0.0055	0.4714286	0.0942857	–
7	0.001	0.0857143	0.0171429	–
17	0.055	4.7142857	0.9428571	+
21	0.01	0.8571429	0.1714286	–
29	0.0001	0.0085714	0.0017143	–
37	0.055	4.7142857	0.9428571	+
39	0.01	0.8571429	0.1714286	–
40	0.001	0.0857143	0.0171429	–
58	0.0055	0.4714286	0.0942857	–
62	0.0001	0.0085714	0.0017143	–
66	0.001	0.0857143	0.0171429	–
72	0.01	0.8571429	0.1714286	–

[a] +, positive; −, negative.

APPENDIX C

RV serotypes and isolates potentially detected by the Pic-5 MGB probe as of July 2005

Appendix C

RV serotype or isolate	GenBank accession no.
Serotypes in GenBank detected by Pic-5 in this study with perfect sequence alignment with Pic-4	
2	X02316
7	AF108185
21	AF108180
29	AF108181
58	AF108183
62	AF108184
Serotypes in Genbank detected by Pic-5 in this study with mismatches to the Pic-4 sequence	
1A	AF108179
17	AF542419
37	AF108182
39	AY751783
72	AF108186
Serotypes not found in GenBank detected by Pic-5 in this study	
3, 40, 66	Not available
Serotypes in GenBank potentially detected by Pic-5 with perfect sequence alignment	
6	AF542425
14	X01087
52	AF542423
69	AF542426
70	AF542427
85	AF542430
86	AF542431
89	M16248
91	AF542432

Appendix C, continued.

Isolates in GenBank potentially detected by Pic-5 with perfect sequence alignment	
M0107078	AF542433
M4067077	AF542436
M5047007	AF542438
M6037300	AF542440
M6117258	AF542442
92-19168	AF108149
93-04433	AF108151
93-23024	AF108154
93-24070	AF108155
94-08089	AF108157
94-08121	AF108158
94-08854	AF108159
94-09504	AF108161
95-01010	AF108163
95-01468	AF108164
95-01470	AF108166
95-01675	AF108167
95-01841	AF108170
95-03031	AF108174
95-03504	AF108175
95-04750	AF108176
95-05109	AF108178

BIBLIOGRAPHY

1. **Afonina, I., M. Zivarts, I. Kutyavin, E. Lukhtanov, H. Gamper, and R. B. Meyer.** 1997. Efficient priming of PCR with short oligonucleotides conjugated to a minor groove binder. Nucleic Acids Res **25:**2657-60.

2. **Afonina, I. A., M. W. Reed, E. Lusby, I. G. Shishkina, and Y. S. Belousov.** 2002. Minor groove binder-conjugated DNA probes for quantitative DNA detection by hybridization-triggered fluorescence. Biotechniques **32:**940-949.

3. **Andeweg, A. C., T. M. Bestebroer, M. Huybreghs, T. G. Kimman, and J. C. de Jong.** 1999. Improved detection of rhinoviruses in clinical samples by using a newly developed nested reverse transcription-PCR assay. J Clin Microbiol **37:**524-30.

4. **Anzueto, A., and M. S. Niederman.** 2003. Diagnosis and treatment of rhinovirus respiratory infections. Chest **123:**1664-72.

5. **Arruda, E., and F. G. Hayden.** 1993. Detection of human rhinovirus RNA in nasal washings by PCR. Mol Cell Probes **7:**373-9.

6. **Bella, J., and M. G. Rossmann.** 1999. Review: rhinoviruses and their ICAM receptors. J Struct Biol **128:**69-74.

7. **Belsham, G. J., and N. Sonenberg.** 1996. RNA-protein interactions in regulation of picornavirus RNA translation. Microbiol Rev **60:**499-511.

8. **Billaud, G., S. Peny, V. Legay, B. Lina, and M. Valette.** 2003. Detection of rhinovirus and enterovirus in upper respiratory tract samples using a multiplex nested PCR. J Virol Methods **108:**223-8.

9. **Blomqvist, S., A. Skytta, M. Roivainen, and T. Hovi.** 1999. Rapid detection of human rhinoviruses in nasopharyngeal aspirates by a microwell reverse transcription-PCR-hybridization assay. J Clin Microbiol **37:**2813-6.

10. **Coiras, M. T., J. C. Aguilar, M. L. Garcia, I. Casas, and P. Perez-Brena.** 2004. Simultaneous detection of fourteen respiratory viruses in clinical specimens by two multiplex reverse transcription nested-PCR assays. J Med Virol **72:**484-95.

11. **Colonno, R. J., J. H. Condra, S. Mizutani, P. L. Callahan, M. E. Davies, and M. A. Murcko.** 1988. Evidence for the direct involvement of the rhinovirus canyon in receptor binding. Proc Natl Acad Sci U S A **85:**5449-53.

12. **Corless, C. E., M. Guiver, R. Borrow, V. Edwards-Jones, A. J. Fox, E. B. Kaczmarski, and K. J. Mutton.** 2002. Development and evaluation of a 'real-time' RT-PCR for the detection of enterovirus and parechovirus RNA in CSF and throat swab samples. J Med Virol **67:**555-62.

13. **Dagher, H., H. Donninger, P. Hutchinson, R. Ghildyal, and P. Bardin.** 2004. Rhinovirus detection: comparison of real-time and conventional PCR. J Virol Methods **117:**113-21.

14. **Deffernez, C., W. Wunderli, Y. Thomas, S. Yerly, L. Perrin, and L. Kaiser.** 2004. Amplicon sequencing and improved detection of human rhinovirus in respiratory samples. J Clin Microbiol **42:**3212-8.

15. **Fendrick, A. M.** 2003. Viral respiratory infections due to rhinoviruses: current knowledge, new developments. Am J Ther **10:**193-202.

16. **Fernandez, C., D. Boutolleau, C. Manichanh, N. Mangeney, H. Agut, and A. Gautheret-Dejean.** 2002. Quantitation of HHV-7 genome by real-time polymerase chain reaction assay using MGB probe technology. J Virol Methods **106:**11-6.

17. **Greisen, K., M. Loeffelholz, A. Purohit, and D. Leong.** 1994. PCR primers and probes for the 16S rRNA gene of most species of pathogenic bacteria, including bacteria found in cerebrospinal fluid. J Clin Microbiol **32:**335-51.

18. **Gwaltney, J. M.** 2002. Clinical significance and pathogenesis of viral respiratory infections. Am J Med **112 Suppl 6A:**13S-18S.

19. **Halonen, P., E. Rocha, J. Hierholzer, B. Holloway, T. Hyypia, P. Hurskainen, and M. Pallansch.** 1995. Detection of enteroviruses and rhinoviruses in clinical specimens by PCR and liquid-phase hybridization. J Clin Microbiol **33:**648-53.

20. **Hamparian, V. V., R. J. Colonno, M. K. Cooney, E. C. Dick, J. M. Gwaltney, Jr., J. H. Hughes, W. S. Jordan, Jr., A. Z. Kapikian, W. J. Mogabgab, A. Monto, and et al.** 1987. A collaborative report: rhinoviruses--extension of the numbering system from 89 to 100. Virology **159:**191-2.

21. **Hayden, F. G.** 2004. Rhinovirus and the lower respiratory tract. Rev Med Virol **14:**17-31.

22. **Heikkinen, T., and A. Jarvinen.** 2003. The common cold. Lancet **361:**51-9.

23. **Hirst, G. K., and M. W. Pons.** 1973. Mechanism of influenza recombination. II. Virus aggregation and its effect on plaque formation by so-called noninfective virus. Virology **56:**620-31.

24. **Hu, W., B. Bai, Z. Hu, Z. Chen, X. An, L. Tang, J. Yang, H. Wang, and H. Wang.** 2005. Development and evaluation of a multitarget real-time Taqman reverse transcription-PCR assay for detection of the severe acute respiratory syndrome-associated

coronavirus and surveillance for an apparently related coronavirus found in masked palm civets. J Clin Microbiol **43:**2041-6.

25. **Hyypia, T., P. Auvinen, and M. Maaronen.** 1989. Polymerase chain reaction for human picornaviruses. J Gen Virol **70 (Pt 12):**3261-8.

26. **Hyypia, T., T. Puhakka, O. Ruuskanen, M. Makela, A. Arola, and P. Arstila.** 1998. Molecular diagnosis of human rhinovirus infections: comparison with virus isolation. J Clin Microbiol **36:**2081-3.

27. **Ison, M. G., F. G. Hayden, L. Kaiser, L. Corey, and M. Boeckh.** 2003. Rhinovirus infections in hematopoietic stem cell transplant recipients with pneumonia. Clin Infect Dis **36:**1139-43.

28. **Jensen, J. S., E. Bjornelius, B. Dohn, and P. Lidbrink.** 2004. Use of TaqMan 5' nuclease real-time PCR for quantitative detection of Mycoplasma genitalium DNA in males with and without urethritis who were attendees at a sexually transmitted disease clinic. J Clin Microbiol **42:**683-92.

29. **Johnston, S. L., G. Sanderson, P. K. Pattemore, S. Smith, P. G. Bardin, C. B. Bruce, P. R. Lambden, D. A. Tyrrell, and S. T. Holgate.** 1993. Use of polymerase chain reaction for diagnosis of picornavirus infection in subjects with and without respiratory symptoms. J Clin Microbiol **31:**111-7.

30. **Kammerer, U., B. Kunkel, and K. Korn.** 1994. Nested PCR for specific detection and rapid identification of human picornaviruses. J Clin Microbiol **32:**285-91.

31. **Kares, S., M. Lonnrot, P. Vuorinen, S. Oikarinen, S. Taurianen, and H. Hyoty.** 2004. Real-time PCR for rapid diagnosis of entero- and rhinovirus infections using LightCycler. J Clin Virol **29:**99-104.

32. **Kutyavin, I. V., I. A. Afonina, A. Mills, V. V. Gorn, E. A. Lukhtanov, E. S. Belousov, M. J. Singer, D. K. Walburger, S. G. Lokhov, A. A. Gall, R. Dempcy, M. W. Reed, R. B. Meyer, and J. Hedgpeth.** 2000. 3'-minor groove binder-DNA probes increase sequence specificity at PCR extension temperatures. Nucleic Acids Res **28:**655-61.

33. **Lai, K. K., L. Cook, S. Wendt, L. Corey, and K. R. Jerome.** 2003. Evaluation of real-time PCR versus PCR with liquid-phase hybridization for detection of enterovirus RNA in cerebrospinal fluid. J Clin Microbiol **41:**3133-41.

34. **Lew, A. E., R. E. Bock, J. B. Molloy, C. M. Minchin, S. J. Robinson, and P. Steer.** 2004. Sensitive and specific detection of proviral bovine leukemia virus by 5' Taq nuclease PCR using a 3' minor groove binder fluorogenic probe. J Virol Methods **115:**167-75.

35. **Lin, H. H., S. J. Wang, Y. C. Liu, S. S. Lee, C. K. Hwang, Y. S. Chen, S. R. Wann, and Y. L. Shih.** 2004. Quantitation of severe acute respiratory syndrome coronavirus

genome by real-time polymerase chain reaction assay using minor groove binder DNA probe technology. J Microbiol Immunol Infect **37:**258-65.

36. **Loens, K., M. Ieven, D. Ursi, C. De Laat, P. Sillekens, P. Oudshoorn, and H. Goossens.** 2003. Improved detection of rhinoviruses by nucleic acid sequence-based amplification after nucleotide sequence determination of the 5' noncoding regions of additional rhinovirus strains. J Clin Microbiol **41:**1971-6.

37. **Monpoeho, S., A. Dehee, B. Mignotte, L. Schwartzbrod, V. Marechal, J. C. Nicolas, S. Billaudel, and V. Ferre.** 2000. Quantification of enterovirus RNA in sludge samples using single tube real-time RT-PCR. Biotechniques **29:**88-93.

38. **Monto, A. S.** 2002. The seasonality of rhinovirus infections and its implications for clinical recognition. Clin Ther **24:**1987-97.

39. **Nijhuis, M., N. van Maarseveen, R. Schuurman, S. Verkuijlen, M. de Vos, K. Hendriksen, and A. M. van Loon.** 2002. Rapid and sensitive routine detection of all members of the genus enterovirus in different clinical specimens by real-time PCR. J Clin Microbiol **40:**3666-70.

40. **Ott, S. J., M. Musfeldt, U. Ullmann, J. Hampe, and S. Schreiber.** 2004. Quantification of intestinal bacterial populations by real-time PCR with a universal primer set and minor groove binder probes: a global approach to the enteric flora. J Clin Microbiol **42:**2566-72.

41. **Papadopoulos, N. G., and S. L. Johnston.** 2004. Rhinoviruses. *In* J. E. B. Arie J. Zuckerman, John R. Pattison, Paul D. Griffiths, Barry D. Schoub (ed.), Principles and Practice of Clinical Virology, 5th ed. John Wiley & Sons, Ltd.

42. **Patterson, L. J., and V. V. Hamparian.** 1997. Hyper-antigenic variation occurs with human rhinovirus type 17. J Virol **71:**1370-4.

43. **Pitkaranta, A., E. Arruda, H. Malmberg, and F. G. Hayden.** 1997. Detection of rhinovirus in sinus brushings of patients with acute community-acquired sinusitis by reverse transcription-PCR. J Clin Microbiol **35:**1791-3.

44. **Reed, L. J., and H. Muench.** 1938. A simple method of estimating fifty per cent endpoints. Am J Hyg **27:**493-497.

45. **Register, R. B., C. R. Uncapher, A. M. Naylor, D. W. Lineberger, and R. J. Colonno.** 1991. Human-murine chimeras of ICAM-1 identify amino acid residues critical for rhinovirus and antibody binding. J Virol **65:**6589-96.

46. **Rossmann, M. G., J. Bella, P. R. Kolatkar, Y. He, E. Wimmer, R. J. Kuhn, and T. S. Baker.** 2000. Cell recognition and entry by rhino- and enteroviruses. Virology **269:**239-47.

47. **Rossmann, M. G., and A. C. Palmenberg.** 1988. Conservation of the putative receptor attachment site in picornaviruses. Virology **164:**373-82.

48. **Savolainen, C., S. Blomqvist, and T. Hovi.** 2003. Human rhinoviruses. Paediatr Respir Rev **4:**91-8.

49. **Skern, T., W. Sommergruber, D. Blaas, P. Gruendler, F. Fraundorfer, C. Pieler, I. Fogy, and E. Kuechler.** 1985. Human rhinovirus 2: complete nucleotide sequence and proteolytic processing signals in the capsid protein region. Nucleic Acids Res **13:**2111-26.

50. **Steininger, C., S. W. Aberle, and T. Popow-Kraupp.** 2001. Early detection of acute rhinovirus infections by a rapid reverse transcription-PCR assay. J Clin Microbiol **39:**129-33.

51. **Sylvain, K., H. Aurelie, M. Marc, and R. Christophe.** 2004. Rapid screening for HLA-B27 by a TaqMan-PCR assay using sequence-specific primers and a minor groove binder probe, a novel type of TaqMan trade mark probe. J Immunol Methods **287:**179-86.

52. **van Elden, L. J., M. G. van Kraaij, M. Nijhuis, K. A. Hendriksen, A. W. Dekker, M. Rozenberg-Arska, and A. M. van Loon.** 2002. Polymerase chain reaction is more sensitive than viral culture and antigen testing for the detection of respiratory viruses in adults with hematological cancer and pneumonia. Clin Infect Dis **34:**177-83.

53. **Van Hoeyveld, E., F. Houtmeyers, C. Massonet, L. Moens, M. Van Ranst, N. Blanckaert, and X. Bossuyt.** 2004. Detection of single nucleotide polymorphisms in the mannose-binding lectin gene using minor groove binder-DNA probes. J Immunol Methods **287:**227-30.

54. **van Kraaij, M. G., L. J. van Elden, A. M. van Loon, K. A. Hendriksen, L. Laterveer, A. W. Dekker, and M. Nijhuis.** 2005. Frequent detection of respiratory viruses in adult recipients of stem cell transplants with the use of real-time polymerase chain reaction, compared with viral culture. Clin Infect Dis **40:**662-9.

55. **Wada, T., S. Maeda, A. Tamaru, S. Imai, A. Hase, and K. Kobayashi.** 2004. Dual-probe assay for rapid detection of drug-resistant Mycobacterium tuberculosis by real-time PCR. J Clin Microbiol **42:**5277-85.

56. **Walburger, D. K., I. A. Afonina, and R. Wydro.** 2001. An improved real time PCR method for simultaneous detection of C282Y and H63D mutations in the HFE gene associated with hereditary hemochromatosis. Mutat Res **432:**69-78.

57. **Wald, T. G., P. Shult, P. Krause, B. A. Miller, P. Drinka, and S. Gravenstein.** 1995. A rhinovirus outbreak among residents of a long-term care facility. Ann Intern Med **123:**588-93.

58. **Wat, D.** 2004. The common cold: a review of the literature. Eur J Intern Med **15:**79-88.

59. **Yoshitomi, K. J., K. C. Jinneman, and S. D. Weagant.** 2003. Optimization of a 3'-minor groove binder-DNA probe targeting the uidA gene for rapid identification of Escherichia coli O157:H7 using real-time PCR. Mol Cell Probes **17:**275-80.

60. **Zhao, J. R., Y. J. Bai, Q. H. Zhang, Y. Wan, D. Li, and X. J. Yan.** 2005. Detection of hepatitis B virus DNA by real-time PCR using TaqMan-MGB probe technology. World J Gastroenterol **11:**508-10.